Inorganic Chemistry, Vol. 17, No. 9, 1978 **2553**

Contribution from the Department of Chemistry,
Cornell University, Ithaca, New York 14853

Eight-Coordination

JEREMY K. BURDETT,[1] ROALD HOFFMANN,* and ROBERT C. FAY

Received April 14, 1978

A systematic molecular orbital analysis of eight-coordinate molecules is presented. The emphasis lies in appreciating the basic electronic structure, σ and π substituent site preferences, and relative bond lengths within a particular geometry for the following structures: dodecahedron (DD), square antiprism (SAP), C_{2v} bicapped trigonal prism (BTP), cube (C), hexagonal bipyramid (HB), square prism (SP), bicapped trigonal antiprism (BTAP), and D_{3h} bicapped trigonal prism (ETP). With respect to σ or electronegativity effects the better σ donor should lie in the A sites of the DD and the capping sites of the BTP, although the preferences are not very strong when viewed from the basis of ligand charges. For d^2 π acceptors and d^0 π donors, π site preferences are $\perp_B > \perp_A > \|_{A,B}$ (> means better than) for the DD (this is Orgel's rule), $\| > \perp$ for the SAP, $(m_\| \sim b_\|) > b_\perp > (c_\| \sim c_\perp \sim m_\perp)$ for the BTP (b, c, and m refer to ligands which are basal, are capping, or belong to the trigonal faces and lie on a vertical mirror plane) and $eq_\| \sim ax > eq_\perp$ for the HB. The reverse order holds for d^2 donors. The observed site preferences in the DD are probably controlled by a mixture of steric and electronic (σ, π) effects. An interesting crossover from $r(M-A)/r(M-B) > 1$ to $r(M-A)/r(M-B) < 1$ is found as a function of geometry for the DD structure which is well matched by experimental observations. Similar effects should occur in the BTP structure, but here experimental data are scarce. The importance of electronic effects in the form of metal–ligand interactions in stabilizing a particular geometry is estimated by using perturbation theory in the form of the angular overlap method (AOM). In order of increasing energy ETP < BTP < SAP < DD ≪ C ~ HB ~ BTAP. The importance of steric effects is estimated by calculating the energy of an L_8^{8-} species by molecular orbital methods. In order of increasing energy DD ~ SAP < BTP ~ C < HB ~ BTAP ≪ ETP. The combination of these two series leads to an explanation of the relative popularity of these structures, DD, SAP, BTP ≫ C, HB, BTAP ≫ ETP. The importance of the low-symmetry BTP as a low-energy structure for the d^0 configuration clearly emerges. The perturbation theory approach is also used to rationalize the relative bond lengths in the DD structure as a function of geometry and in the bipyramidal 5-, 7-, and 8-coordinate structures. Polytopal rearrangements are found to be barrierless from MO calculations on systems with nonchelating ligands for at least one pathway between DD and SAP or from either of these structures to the BTP geometry.

Eight-coordination[2] is common in the structures of ionic solids, metals, and alloys. For example, the Ca^{2+} ion in fluorite and the Cs^+ ion in CsCl are both eight-coordinated in the form of a cube. If we exclude these systems and also metal cluster complexes, we are still left with a wide range of discrete complexes and polymeric systems based on the coordination number 8.

There are many examples of eight-coordination to be found in the chemistry of the early transition metals and the actinides and lanthanides. For Ln(III) 8 is the most common coordination number in complexes. (We will use the symbols Ln and An to denote lanthanide and actinide metals, respectively.) The structures of the lanthanide silicates[3] are polymeric, containing SiO_4 tetrahedra, the oxygen atoms of which are often arranged so as to eight-coordinate the metal ion. These polyhedra are usually very distorted in terms of both angular geometry and the spread of M–O distances. This coordination number is also prevalent among the fluorides of the actinide elements, where monomeric, chain, and sheet structures based on eight-coordinate polyhedra are found.[4] Eight-coordination is most frequently found at the left-hand side of the transition-metal series and with d^2, d^1, or d^0 electronic configuration, although a few examples with a greater number of d electrons are known.

One way of viewing the various eight-coordinate geometries we shall discuss here is to trace, conceptually, their descent from two six-coordinate forms, the octahedron and the trigonal prism. This is done in Figure 1, which also sets the mnemonic nomenclature we shall use to describe the various structures. Examples are known of almost all of these geometries and also of many structures intermediate between two idealized extremes. We take the opportunity here to point out that for many of the experimental structures it is difficult to readily describe their geometry. The phrases "distorted dodecahedron" or "approximately square antiprismatic" are often encountered in the literature. While the methods of Porai-Koshits and Aslanov[5] and of Muetterties and Guggenberger[6] are now available to describe the direction and degree of such distortions, the bulk of the literature still contains the earlier more imprecise language.

The geometrical distortions required to send one structure into another are often rather small. We show the connection between the hexagonal bipyramid (HB), the bicapped trigonal antiprism (BTAP), and the cube (C) in **1**. The cube may

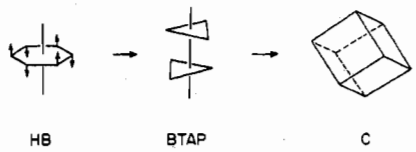

1

distort in several other ways as well. By elongation or compression along one fourfold axis a square prism (SP) is produced. By rotation of the upper four ligands around one fourfold axis relative to the lower set a square antiprism (SAP) is produced. The dodecahedron (DD) may be produced by a puckering motion, as shown in **2**. In this important geometry there are two symmetry-unrelated sites, conventionally labeled A and B.

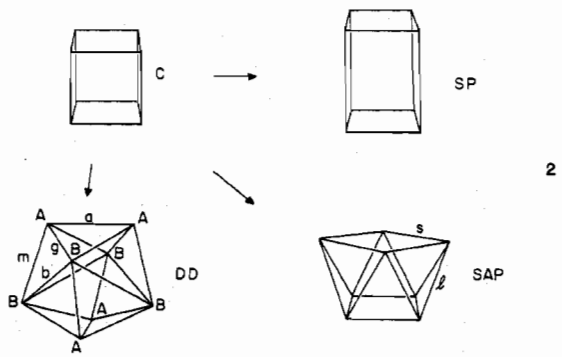

2

The SAP may distort to the C_{2v} bicapped trigonal prism (BTP), as shown in **3**. The latter polyhedron has three different ligand sites, those which we call basal (b), those which

0020-1669/78/1317-2553$01.00/0

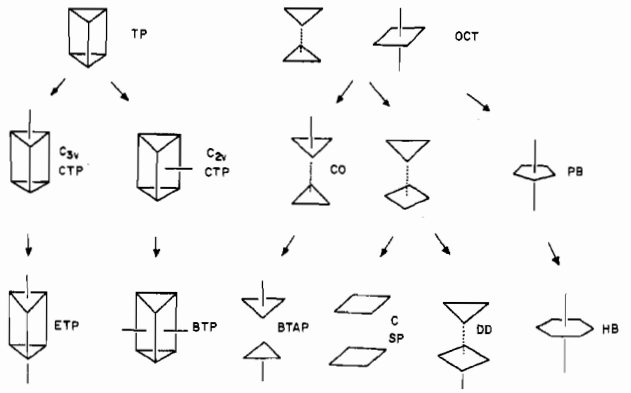

Figure 1. Schematic hierarchy of six-, seven-, and eight-coordinate geometries.

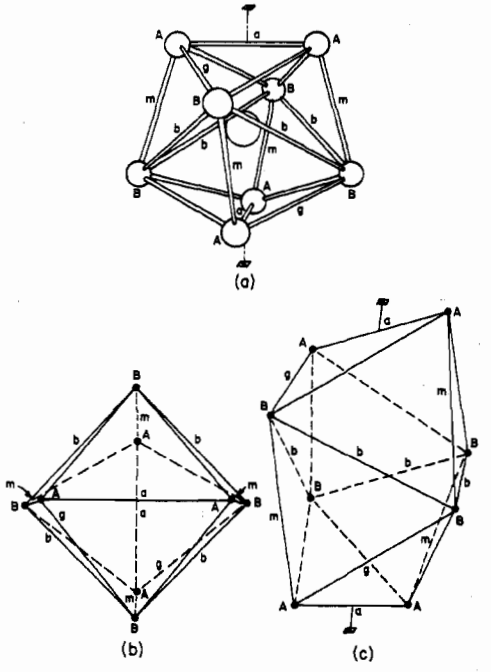

Figure 2. Three views of the DD: (a) the usual openwork view; (b) a view taken down the $\bar{4}$ axis which emphasizes the relationship to the C and SAP; (c) a view taken approximately down one of the twofold axes emphasizing the relationship to the BTP.

we call capping (c), and those which lie in the vertical mirror plane (m).

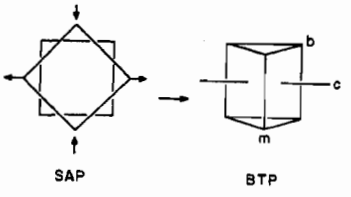

3

In addition to viewing the DD as a bicapped octahedron as in Figure 1, the three views of the dodecahedron in Figure 2 show its relationship to the BTP and SP. Thus the BTP is a way-point between the DD and SAP structures. Another way to interconnect the two is via a rotation and relaxation about the fourfold axis of the SAP (**4** → **5**) or about the $\bar{4}$ axis of the DD (**5** → **4**). There is, of course, no differentiation between the A and B sites of the DD after the rotation to the SAP. Still a third route is the square face–diamond face interconversion shown in **6**. This may also be viewed as the rotation of pairs of A and B ligands against each other.[7c]

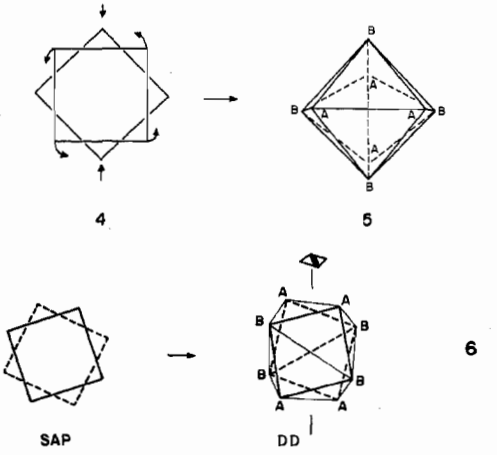

Muetterties and Wright in their review[2a] on high coordination numbers divided the idealized eight-coordinate geometries into two groups, a low-energy set of structures (DD, SAP, BTP) and a higher energy set (BTAP, C, SP, HB). There is a relatively small number of examples of these high-energy structures if we exclude the rather special case of HB's containing the uranyl ion. By far the largest number of structural examples are found for the DD and SAP geometries, many with chelating ligands. Often there are alternative chelation modes, and we note here that the preferred isomer will be determined by a delicate balance of a host of electronic, "bite-size", steric, and packing effects. Indeed, structural preferences for monodentate ligand systems will be influenced by these same effects.

Hoard and Silverton[8] in a classic paper have discussed eight-coordinate polyhedra with respect to three main points: (a) direct bonding between the central atom and the ligands, (b) mutual repulsions by the ligands, and (c) geometrical constraints exerted by polydentate ligands. The role of (b) was estimated by examining the energy of eight points constrained to move on the surface of a sphere subject to a repulsive potential $\sum_{i \neq j} r_{ij}^{-n}$, where r_{ij} is the distance between two points i and j. For $n \rightarrow \infty$ we have the hard-sphere model. Softer potentials with values of n between 1 (Coulombic) and 6 were also used. For the DD structure the geometry was allowed to relax further by letting the A and B ligands move on different concentric spheres. The most favorable polyhedron for any value of n for monodentate ligands is the SAP, though dodecahedra are not much higher in energy. For small-bite bidentate ligands, however, the DD structure was preferred. Kepert[7] has extended this approach[9] and looked at the interconversion of the two geometries. For the coordinate **6**[7c] there was virtually no energy change on going from the DD to the SAP structure.

The following sections contain a systematic molecular orbital analysis of the several eight-coordinate structures. The extended Hückel method is used, with parameters specified in the Appendix. For many of these geometries the d orbital region of the molecular orbital diagram has been derived previously using crystal field and ligand field approaches.[10,11] In addition to probing substituent site preferences, we shall also attempt to separate the competing effects of steric and electronic influences in determining the geometries of eight-coordinate systems.

The Basic Eight-Coordinate Geometries

In this section we follow a line of attack similar to that used previously in the analysis of five-[12] and seven-coordination,[13] that is, to explore the basic features of the molecular orbital diagrams of the various geometries and to derive therefrom the site preferences of substituents distinguished by their σ-donating or -accepting ability. The role of π effects will be

explored separately. We report in this section calculations primarily for ML_8, where L is a pseudoligand bearing only a single σ orbital. Also calculated are energies for L_8^{8-}, without the central atom, in an attempt to explore the steric demands of each structure, and energies for the more realistic systems MCl_8 and $M(CO)_8$. In a later section we will delve deeper into the significance and derivation of the population analyses reported, and we will attempt there to separate the steric and electronic controls on the molecular geometry. Remembering the Muetterties and Wright[2a] separation of the structures into those which were stable and those which were not, we begin by looking at those systems which are felt to be at rather high energy.

Hexagonal Bipyramid (HB) and Bicapped Trigonal Antiprism (BTAP). The level ordering for these two geometries is shown in **7**. For the HB the low-lying e_{1g} set is not involved

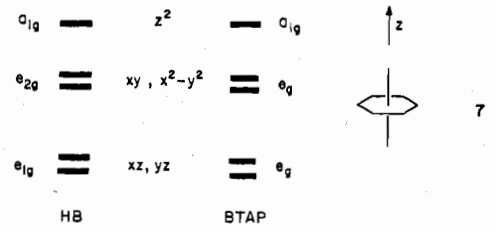

7

in σ bonding at all. The general level pattern resembles that for both five- and seven-coordinate bipyramidal geometries.[12,13] As in the seven-coordinate case, the second degenerate set (e_{2g}) is of the wrong symmetry to interact with and be stabilized by $(n + 1)$ p orbitals. There is therefore a large energy gap between e_{1g} and e_{2g}. On distorting the HB toward a BTAP the two degenerate pairs lose their 1,2 labels and mix together. As a result, the lower e set remains σ nonbonding and equienergetic throughout this distortion. The upper e set rises in energy, eventually to coalesce with the a_{1g} orbital at the cube geometry (**1**). For all the systems that we have studied [d^0 and d^2 ML_8, L_8^{8-}, MCl_8, and $M(CO)_8$] this distortion coordinate contains a minimum at the cubical geometry.

The population analysis given in **8** for the HB holds for d^0

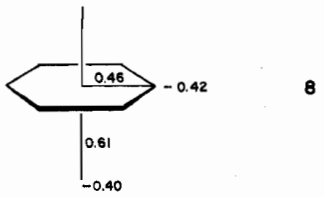

8

through low-spin d^4 configurations. There is little preference on electronegativity grounds for either axial or equatorial sites. The axial bonds, however, are predicted to be substantially stronger than the equatorial ones. The reason for this will be discussed later. As the equatorial belt is puckered and the molecule distorts to the cube, the axial overlap populations decrease considerably and the equatorial ones increase by a smaller amount to a common value of 0.52.

Most of the examples showing the HB geometry contain UO_2 or another AnO_2 unit along the axis.[14] Very short axial U–O bonds are found, and as in the seven-coordinate case, these are probably due to the strong σ bonding and also the excellent arrangement for M–axial ligand π bonding. The HB geometry is not limited to systems containing AnO_2. For example, the β modification of YSF contains[15] HB's with six equatorial F atoms and two axial S atoms coordinating the Y. However, the structure of $UCl_2(Me_2SO)_6^{2+}$ which one might have anticipated would be a HB with axial chlorines assumes instead a dodecahedral structure with Cl atoms in the B sites (see below), such that the Cl–U–Cl is 91°. An alternative structure where the two Cl atoms are arranged so as to give a Cl–U–Cl angle much nearer linearity is not observed either.

Square Prism (SP). The cube, O_h, in addition to being reached by puckering of the HB via a BTAP, is a part of another natural distortion coordinate—that of the D_{4h} square prism. In **9** we show the evolution of the cube levels as it is

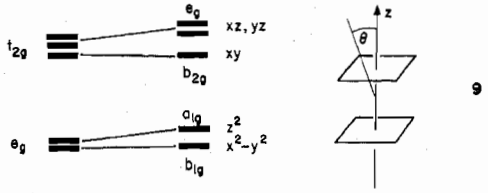

9

distorted to a square prism. The deformation may be measured by the polar angle θ. The cube is defined by $\theta = \cos^{-1}(1/3^{1/2}) = 54.73°$ and the drawing shows the splitting pattern for $\theta < \theta$(cube). At the cubical geometry each ligand σ orbital precisely hits the node in z^2 (**10**), leaving it nonbonding.

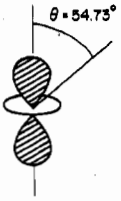

10

Distortion on either side of $\theta = \theta$(cube) leads to an increase in the energy of z^2. The population analysis for an ML_8 cubic geometry is given in **11**.

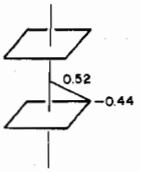

11

We find the cube to be the lowest energy geometry within this D_{4h} deformation coordinate for all d^0–d^4 systems studied. There is an example of a nearly cubic geometry in a discrete transition-metal complex in $Et_4U(NCS)_8$.[17a] The N–U–N angles are found with two different values, 70.3 and 71.1°, very close to the 70.5° expected for the perfect cube. [Interestingly, in $Cs_4U(NCS)_8$[17b] the coordination around the uranium is SAP.] In Na_3PaF_8 one finds[18] a SP with $\theta = 56°$, only slightly distorted from the cube, with edges parallel to the fourfold axis of 2.47 Å and perpendicular to it of 2.60 Å. The only other example of (approximate) molecular cubic coordination we have been able to find is that of $U(bpy)_4$.[19] Cubic coordination is often found in ionic solid-state structures, for example, CaF_2. Many other compounds, e.g., MO_2 (M = Pa, Np, Pu, Am),[20] have this structure, but it is probably not legitimate to refer these to isolated MX_8 cubic geometries. Also many distorted cubic structures may be found among other actinide complexes. A slightly distorted cubic geometry is also found for ammonium and alkali metal complexes with the "wraparound" ligands tetranactin and nonactin, respectively, cyclic polyethers which also contain carbonyl groups. In the fascinating structure of K^+ (nonactin)[21a] and NH_4^+ (tetranactin)[21b] four carbonyl O atoms and four ether O atoms coordinate the central ion in the form of a cube. We also note here that the cube geometry is an observed arrangement for polyhedral molecules such as cubane.

End-Bicapped Trigonal Prism (ETP). This is predicted to be a high-energy structure. In fact Hoard and Silverton say[8] this is "sterically so obviously inferior to the cube as scarcely to merit consideration", but we have a reason for retaining it here, which will become clear below. The ETP level ordering is shown in **12** for $\theta = 58°$, where a minimum in energy occurs

12

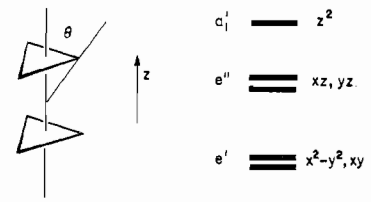

for L_8^{8-} and ML_8. The orbital ordering is similar to that reported for the end-capped trigonal prism in the seven-coordinate case. The e'' set is pushed to high energy by σ interaction, and the p orbitals do not have the correct symmetry to depress it. Stabilization of this sort does occur with the lower energy e' set, which is also destabilized by interaction with the ligand σ functions. Analogously with the seven-coordinate C_{3v} capped prism[13] the ETP is stabilized considerably on removal of electrons from these e' orbitals to become closer in energy for the d^0 configuration to the cube and HB structures.

A few possible examples of this structure are known, although sometimes it is debatable whether the stucture is six- or eight-coordinate. In $Rb_2Na(hfac)_3$[22a] the O atoms of the ligand coordinate the Na as a trigonal prism, and the two Rb atoms cap the trigonal faces, **13**. The Na–O distance is 2.4

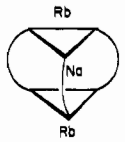

13

Å and the Na–Rb distance, calculated by us, is 3.7 Å. Data for the Rb_2 or NaRb molecules are unavailable, but the bond length[23] in the K_2 molecule is 3.92 Å and that in Na_2 3.08 Å, which suggests that some Rb–Na interaction is possible. Perhaps a more persuasive ETP structure is found in complexes[22b] of the alkali metal ions with the macrobicyclic diamino hexaether "football" ligand $C_{18}H_{36}N_2O_6$. Here the six O atoms form a structure somewhere between a trigonal prism and a trigonal antiprism and the two N atoms cap the trigonal faces. The M–N and M–O distances in this system are comparable. The best approximation to the ETP structure is for M = Cs, Rb where the twist angle between the two trigonal planes is 15° (0° for ETP, 60° for BTAP).

The population analysis, **14**, suggests that the axial bonds

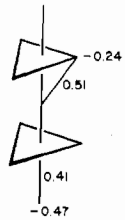

14

should be weaker than the others but indicates that the better σ-electron-acceptor (more electronegative) ligand should go in the axial site, which is not the case in **13**. The central atom here (Na), however, has no accessible d orbitals. A calculation on this system gives only a slight difference in atomic charges and an extremely weak axial bond compared to that of the others. This is certainly in accord with the observed structure.

Each of the foregoing structures contained at its equilibrium geometry a low-energy pair of d orbitals, which could readily accommodate four electrons. With eight two-electron donor ligands this gives a total electron count of 20. More stable structures should be those where a single d orbital lies to low energy. All of the structures that follow exhibit this feature and are more stable for all configurations d^0–d^2. They share the common property of a large energy gap between this low-lying level and the next.

Table I. Central Atom s, p, and d and Ligand σ Combinations for Eight-Coordinate Geometries

polyhedron	point group	d					p			s
		z^2	x^2-y^2	xy	xz	yz	x	y	z	
DD	D_{2d}	a_1	b_1	b_2	e		e		b_2	a_1
SAP	D_{4d}	a_1	e_2		e_3		e_1		b_2	a_1
SP	D_{4h}	a_{1g}	b_{1g}	b_{2g}	e_g		e_u		a_{2u}	a_{1g}
C	O_h	e_g			t_{2g}		t_{1u}			a_{1g}
HB	D_{6h}	a_{1g}	e_{2g}		e_{1g}		e_{1u}		a_{2u}	a_{1g}
BTAP	D_{3d}	a_{1g}	e_g		e_g		e_u		a_{2u}	a_{1g}
ETP	D_{3h}	a_1'	e'		e''		e''		a_2''	a_1'
BTP	C_{2v}	a_1	a_1	a_2	b_1	b_2	b_1	b_2	a_1	a_1

DD $2a_1 + 2b_2 + 2e$

SAP $a_1 + b_2 + e_1 + e_2 + e_3$

SP $a_{1g} + b_{1g} + e_g + b_{2u} + a_{2u} + e_u$

C $a_{1g} + t_{2g} + a_{2u} + t_{1u}$

HB $2a_{1g} + a_{2u} + b_{1u} + e_{2g} + e_{1u}$

BTAP $2a_{1g} + e_g + 2a_{2u} + e_u$

ETP $2a_1' + 2a_2'' + e' + e''$

BTP $3a_1 + a_2 + 2b_1 + 2b_2$

Another prominent result of the calculations above on the HB and the SP is the presence of a ligand combination at high energy which is of the wrong symmetry to interact with any of the central metal s, p, or d orbitals. In the HB, for example, it looks like **15**. In our calculations this orbital actually comes

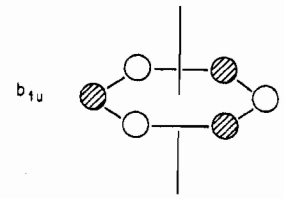

15

above the lowest d-orbital set. To involve this combination in bonding one could invoke metal f orbitals. There might be some justification for doing so in the actinide or lanthanide series, but we would not like to enter this contentious area at this time. In Table I we show the symmetry species of allowed ligand σ combinations (at bottom) and the representations subduced by the metal s, p, and d orbitals (at top). For all of the structures discussed next each ligand representation has a central atom counterpart.

Dodecahedron (DD). A large variety of structures are known with this geometry. The classic $Mo(CN)_8^{4-}$ structure in $K_4Mo(CN)_8 \cdot 2H_2O$ determined many years ago by Hoard and co-workers[24] was the first of many examples. This structure is found for several complexes containing the "small-bite" ligands O_2^{2-} (e.g., $K_3Cr^V(O_2)_4$[10i] and NO_3^- (e.g., $Mn^{II}(NO_3)_4^{2-}$).[25] For small-bite ligands Kepert[7] predicted that the DD structure should be significantly stabilized relative to the SAP. The DD forms the basis of the Th_3P_4 structure[26] which in addition to describing several phosphide systems is also found for a series of alloys, e.g., $La_4Rh_{\sim 3}$.[27] As well as rather complex dodecahedral structures [for example, the HfO_8 unit in $Hf_{18}O_{10}(OH)_{26}(SO_4)_{13}(H_2O)_{33}$[28]] many simpler structures are well characterized, typically containing the bidentate β-diketonate, monothiocarbamate, and dithiocarbamate ligands.

In the molecular orbital diagram for the DD a single σ nonbonding orbital, $x^2 - y^2$, lies to low energy. There have been several orbital descriptions of this structure.[10] The exact ordering of the levels other than the $x^2 - y^2$ depends upon the geometry—that shown in **16** is obtained for $\theta_A = 35°$, $\theta_B =$

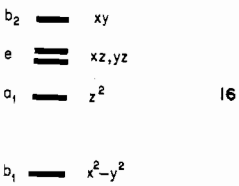

16

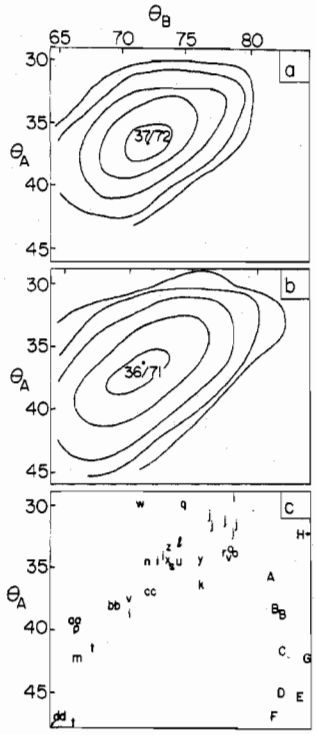

Figure 3. (a) Potential energy surface for the DD L_8^{8-} system. The energy minimum is at θ_A, θ_B = 37°, 72°. (b) Potential energy surface for a d^2 MCl_8 system. The energy minimum is at θ_A, θ_B = 36°, 71°. Similar surfaces are calculated for ML_8 and $M(CO)_8$. (c) Observed values of θ_A, θ_B for a random selection of DD structures taken from the literature. The letters refer to the references in ref 29.

75°. θ_A and θ_B are the angles between the $\bar{4}$ axis of the idealized DD and the bonds which extend from the metal to the dodecahedral A and B sites, respectively. For d^0 and d^2 systems minimum-energy geometries are located at (θ_A, θ_B) = (36°, 74°) for ML_8, (36°, 71°) for MCl_8, and (38°, 74°) for $M(CO)_8$. The hard-sphere model gives (36.9°, 69.5°) and the softer potential of Hoard and Silverton (35.2°, 73.5°), quite close to our values for the metal-containing complexes and that for L_8^{8-} (37°, 72°).

When we calculate a potential energy surface for a general dodecahedron, varying θ_A and θ_B independently within a D_{2d} constraint, we obtain (Figure 3) for L_8^{8-}, MCl_8, $M(CO)_8$, and ML_8 a surface very much like that observed by Kepert[7] from a molecular mechanics approach. A plot of the observed structures gives a distribution consistent with our surfaces and the softer potentials of the Kepert method. Points labeled with capital letters refer to systems with small-bite ligands, for example, O_2^{2-}, NO_3^-, and OAc^-, which are significantly displaced from the valley. Ones with larger values of θ_A contain more than two d electrons. We will return to these cases later.

The bond overlap populations in the DD are sensitive to the molecular geometry. For ML_8 at the minimum-energy geometry we obtain the population analysis **17**. This suggests

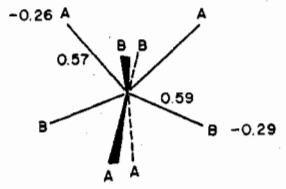

17

that the more electronegative ligands will prefer the B sites and that the stronger σ bonds will be formed between metal and B site ligands. Thus, for equivalent ligands we would

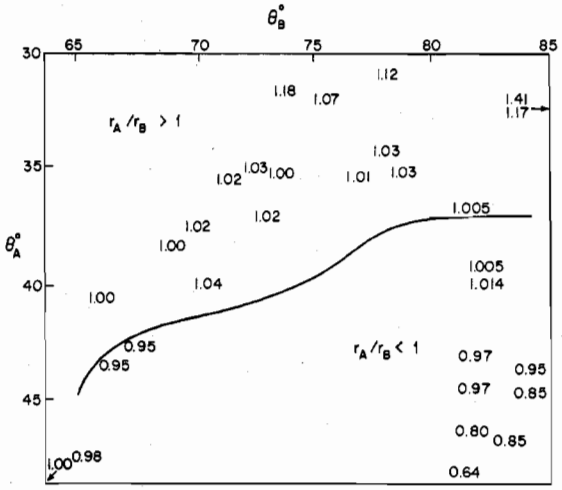

Figure 4. The ratio of bond lengths r_A/r_B for some of the DD molecules of Figure 3c where the A and B sites are occupied by chemically equivalent atoms. The solid line represents the calculated locus of bond overlap population (M–A)/bond overlap population (M–B) = 1 for a d^0 ML_8 system.

expect r(M–A)/r(M–B) > 1. Interestingly, the softer surface of Hoard and Silverton suggested[8] r_A/r_B = 1.03 at the equilibrium geometry, but the spd hybridization approach[10d] of earlier authors found stronger bonding to the ligands in the A sites.

As the geometry is deformed from the minimum in the surface of Figure 3, the relative overlap populations change as shown in Figure 4. On moving from the minimum toward the cube the bond length ratio (r_A/r_B) decreases below unity and then increases to unity again at the cube. We show some r_A/r_B values for several complexes containing identical ligands in Figure 4 and note that there are several structures where the bond length ratio is less than unity. The Swalen and Ibers ligand field calculation[10i] on CrO_8^{3-} (d^1) also showed that for this species r_A/r_B < 1 was to be expected on d orbital grounds alone. Our calculations indicate that above the upper r_A/r_B = unity line of Figure 4 the M–A overlap population increases as θ_A increases, but the M–B overlap population decreases. Below this line both M–A and M–B overlap populations decrease as θ_A decreases. There is as yet insufficient data to test this more detailed result.

There is no change in the site carrying the largest charge in the region covered in Figure 4. The B sites remain more negative throughout. In general the A sites become less negative and the B sites more negative as either θ_A is decreased or θ_B is increased. Thus the difference in the two charges is smallest (–0.25, –0.26) at θ_A = 45°, θ_B = 65°, and largest (–0.19, –0.34) at θ_A = 30°, θ_B = 85°. We note that the difference in charges between the two sites is in fact quite small compared with figures derived previously in geometries with lower coordination numbers. This is a general feature of our study of eight-coordination and suggests that σ site preferences may not be particularly strong if governed by the ligand charge distribution.

In previous work[12,13] we have concentrated exclusively on the charge distribution as a guide to substituent site preferences. An argument could also be made for an analysis based on overlap populations or bond orders—i.e., that the strongest σ donor should enter the site with the largest M–L bond overlap population. The two factors may indeed compete, as they do in this case.

For most geometries the strongest σ donor is expected to reside in the A sites, since these carry the smallest negative charge on the ligand. We should wait until we have discussed π-bonding effects to weight the available data on ligand site

Table II. Site Preferences for Dodecahedral Systems

	A site	B site	d^n	ref
$TiCl_4(diars)_4$	As	Cl	d^0	31
$NbCl_4(diars)_2$	As	Cl	d^1	32
$VCl_4(diars)_2$	As	Cl	d^1	31
$UCl_2(Me_2SO)_6^{2+}$	O	Cl	d^0	16a
$PaOCl_3$	3 Cl, 1 O	2 Cl, 2 O	d^0	16c
$H_4Mo(PPh_3)_4$	H	PPh_3	d^2	30
$Zr(nes)_4$	N	O	d^0	33
$Zr(quin)_4$	N	O	d^0	34
$W(quinBr)_4$	O	N	d^2	35
$Mo(CN)_4(RNC)_4$	CN	RNC	d^2	36
$Zr(NTA)_2^{2-}$	N, O	O	d^0	38
$Zr(edta)\cdot 4H_2O$	2 N, 2 O (H_2O)	4 O	d^0	37
YbO_7Cl[a]	O	Cl, O	d^0	39
$EuCl_2(H_2O)_6^{+}$[b]	O	Cl, O	d^0	40

[a] Part of a large polymeric unit in $Yb_3(SiO_4)_3Cl$. [b] Distorted structure; has this site preference when viewed as DD in $EuCl_3\cdot 6H_2O$.

preferences, but we can take a preliminary look at the situation based on the σ effect alone. In fact most previous arguments as to site preferences have focused on π-type interactions by using Orgel's rule.[10e]

For $H_4Mo(PPh_3)_4$[30] the stronger σ donor (H) goes into the A positions, leaving to the phosphine ligands the sterically more free B sites. This species, with $\theta_A = 30°$, $\theta_B = 71°$, lies off the main sequence of points of Figure 3c (point w). This may simply be due to the steric relaxation of the unbalanced ligand set. Previous analysis[13] of the pentagonal-bipyramidal structure of $H_4Os(PPh_3)_3$ put the H atoms in equatorial sites, where they belonged both sterically and electronically. We have mentioned above that in $UCl_2(Me_2SO)_6^{2+}$[16] the two Cl ligands entered the B sites and the O atoms of the Me_2SO ligand all the A sites and the two B sites remaining, which is the opposite result expected for the more electronegative O ligands. This result is in accord with steric arguments since the larger Cl atom would on those grounds prefer the B sites. In $PaOCl_3$, however, where a dodecahedral PaO_3Cl_5 unit exists, the O and Cl atoms are scattered between the A and B sites. Table II gives some site preferences for a variety of dodecahedral systems. Only in the cases of the d^2 $W(quinBr)_4$[35] and these uranium examples does the σ site guide not apply for good DD geometries. We will return to this point when we consider π bonding in these systems in detail. In several cases not listed in Table I both sorts of atoms in the ligands are found in both A and B sites. These include $Ti^{IV}(mtc)_4$, its Zr(IV) analogue,[41] and $Zr(NO_3)_2(acac)_2$.[42] Here no site preference seems to exist at all.

The DD structure is calculated to be more stable than any of the foregoing ones for the d^0–d^2 configurations. The mean bond overlap population is also larger than for any of the previous structures, indicating an electronic advantage for this geometry. The importance of steric control is also evident from the results of our calculations. For example, as θ_A becomes larger for a given θ_B, the energy increases. We can trace this destabilization to low-lying, mainly ligand, energy levels rising in energy. This is typical of how ligand–ligand repulsions manifest themselves in molecular orbital calculations.

Square Antiprism (SAP). This D_{4d} geometry is also well represented among the known eight-coordinate structures. Whereas $K_4W(CN)_8\cdot 2H_2O$ contains DD $W(CN)_8^{4-}$ ions,[43] in the $H_4W(CN)_8\cdot 6H_2O$ system the SAP structure is found.[44] Similarly the coordination in $Mo(CN)_8^{4-}$ is sensitive to its environment. DD[24] and SAP[45] structures are known. In bis(phthalocyanine) complexes of Sn[47] and U[48] the ligand geometry forces a square-planar arrangement of quartets of coordinating atoms, leading to the SAP structure. In the heteropolytungstate $(W_5O_{18}H)_2Ce^{6-}$ the cerium ion is coordinated[49] by two polytungstate units built from WO_6 octahedra. Four oxygen atoms from each fused unit form a square plane of coordinating ligands. There are also many complexes containing β-diketonate ligands and other chelating ligands. The most common chelation mode is *ssss*.

The orbital splitting pattern for the SAP is shown in **18**.

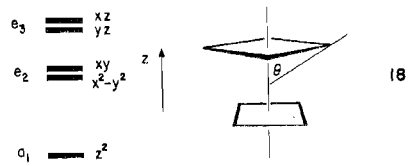

18

The p orbitals transform as $e_1 + b_2$ and so cannot keep the d block e_2 and e_3 orbitals from rising to high energy. The a_1 orbital (z^2) would be σ nonbonding at $\theta = 54.73°$. For larger or smaller θ values it is destabilized. Thus we expect to see a change in equilibrium structure as we move from d^2 to d^0, the former having a θ value closer to 54.73°. For our model system ML_8 we find energy minima at $\theta = 57°$ (d^2) and $\theta = 60°$ (d^0) in accord with this idea, but for the more realistic systems MCl_8 (58°) and $M(CO)_8$ (55°) the changes are imperceptible. For L_8^{8-} itself we find a value of 57°. Experimentally we see an increase in θ on going from d^2 $W(CN)_8^{4-}$ ($\theta_{av} = 57.3°$)[44] to d^1 $W(CN)_8^{3-}$ ($\theta = 59.1°$),[50] but care must be exercised since the former is a distorted structure.[51] The soft- and hard-sphere values are 57.3° and 59.3°, respectively.

Since the lowest energy d orbital is destabilized in this geometry for $\theta \neq 54.73°$ and the lowest energy d orbital in the dodecahedron is purely metal–ligand nonbonding, we might expect an energy advantage for the SAP compared to the DD on going from d^2 via d^1 to d^0 configurations. However, even with the potentially similar species $M(CN)_8^{3-,4-}$ (M = Mo, W), the geometry is very sensitive to crystal environment as we mentioned earlier. In solution the geometry may be cation and solvent dependent.[46]

The population analysis for a SAP with $\theta = 58°$ is given in **19** for the ML_8 system. The figures are comparable with

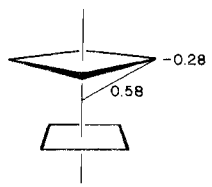

19

those for the DD. Rotation of the two halves of the molecule around the fourfold axis is calculated to be energetically unfavorable, but distortions in this direction are found for several species. The staggering of the two quartets (45° for a perfect SAP) is 38° in $(phth)_2U$ and 42° in $(phth)_2Sn$ (phth = phthalocyanine). Similar distortions are found in $[Sr((NH_2CO)_2NH)_4]^{2+}$[52] and $(PyNO)_8La^{3+}$.[53]

Bicapped Trigonal Prism (BTP). This C_{2v} geometry was first recognized for the YF_3 structure.[54] Subsequently, several species have been found to lie closer to the BTP geometry than the SAP geometry upon close examination. The use of sensitive shape parameters[5,6] has enabled one to obtain a much more definite fix on molecular geometry than was previously possible. For example, the structures of the α forms of $Ce(acac)_4$ and $Th(acac)_4$, recently claimed as mainly dodecahedral, are really better described as BTP.[55]

The level ordering and various electronic effects are best approached by deriving the BTP from an SAP geometry, along the deformation coordinate described earlier in **3**, **20**. Alternatively one could regard the rather low-symmetry geometry as arising via repeated capping of the capped trigonal prism of seven-coordination. From that point of view, shown in **21**,

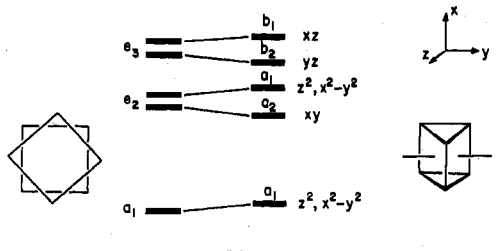

20

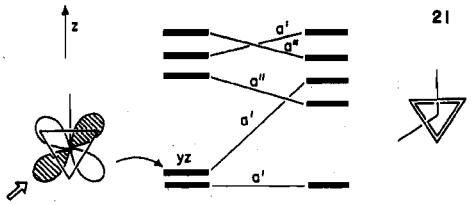

21

the *yz* orbital is ideally disposed in space to interact with the eighth ligand. A feature of our calculation on the BTP that did not arise in previous ligand field calculations is the large energy gap between the lowest energy a_1 orbital and the a_2 orbital above it. The a_1 orbital is a mixture of z^2 and $x^2 - y^2$ and is slightly σ antibonding.

We have optimized the geometry for ML_8 in two ways. First, we have maintained the D_{3h} structure of the six prism ligands and varied the polar angle θ and the angle between the capping ligands α (**22**). The energy minima in this

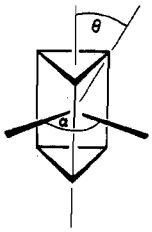

22

coordinate are at $\theta = 49°$, $\alpha = 140°$ (d^2) and $\theta = 45°$, $\alpha = 120°$ (d^0). For the d^0 configuration it is extremely interesting to note that this structure had the lowest energy, by 34 kcal/mol, of any of the geometries studied. In a second geometry optimization procedure the polar angles of all the ligands were varied, with the following C_{2v} constraint [the numbering scheme (of ref 2a) is shown in **23**; θ and φ are

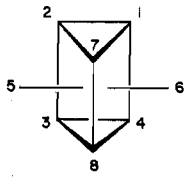

23

defined relative to the *z* and *x* axes of **20**]: $\theta_5 = \theta_6$, $\theta_1 = \theta_2 = \theta_3 = \theta_4$, $\theta_7 = \theta_8$, $\varphi_5 = 0$ ($\varphi_8 = 90$, $\varphi_7 = 270$, $\varphi_6 = 180°$), $\varphi_4 = 180 - \varphi_3$, etc. This distortion coordinate contains the SAP, which for many systems is more stable than the BTP. Thus we searched for the lowest energy structure around the values of θ and φ expected for the BTP. For ML_8 (d^2), $\theta_5 = 69°$, $\theta_8 = 36°$ (fixed), $\theta_3 = 57°$, and $\varphi_3 = 49°$; for ML_8 (d^0), $\theta_5 = 66°$, $\theta_8 = 34°$, $\theta_3 = 57°$, and $\varphi_3 = 49°$. The observation of an energy minimum at a BTP type of geometry for the d^0 ML_8 system is an electronic effect. No minimum is found for L_8^{8-} using the second method. A valley does exist in the potential energy surface connecting the SAP and BTP, the concerted opening out of two ligands and closing in of another two being one of the lowest energy distortions of the L_8^{8-} SAP.

Whichever method of restricted geometry optimization is used, we find an opening out of the angle between the two capping ligands on going from d^0 to d^2. If the D_{3h} prism is maintained for the noncapping ligands, we also see a flattening of this unit on going to d^2. The origin of both these effects may be readily discerned from the form of the lowest energy d orbital. In the case where we retained the D_{3h} geometry of the prism ligands, if the prism axis is designated as *z*, then in this axis system the lowest energy d orbital is a near-equal mixture of z^2 and $x^2 - y^2$ (**24**). Energetically, the flattening of the prism on going from d^0 to d^2 is dominated by the movement of the six prism ligands toward the node of z^2 (**10**) which relieves the destabilizing effect of the out-of-phase mixing of the prism orbitals with the lobe of z^2.

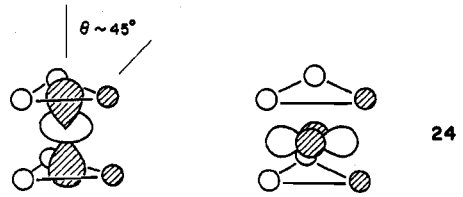

24

In the second minimization procedure one needed to fix θ_7 and θ_8 for the d^2 system; otherwise the BTP immediately distorted to the SAP. The reason for this strong effect may be seen from **25**. On opening out, these two ligands approach

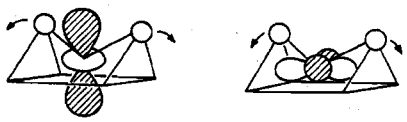

25

the node in z^2 and increase their in-phase interaction with the $x^2 - y^2$ orbital component. The opening out of the capping ligands on going from d^0 to d^2 is a balance of the two effects shown in **26** and is related to those in **25**. The first stabilizes the lowest d orbital on opening up the capping ligands; the second destabilizes it. The former seems to win out. We calculate a much smaller energy change than for **25** in our model ML_8 system.

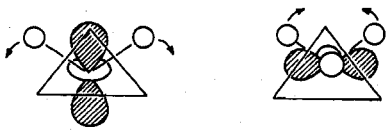

26

For the more realistic ligands MCl_8 and $M(CO)_8$ we do not see a minimum at the BTP for distortions of the second type. The SAP structure is more stable for all electronic configurations, but not by much. Instead we see rather soft distortions of the SAP in the direction of the BTP for d^0 MCl_8 and a minimum somewhere between SAP and BTP structures for d^0 $M(CO)_8$. The minimum at $\theta_5 = 62°$, $\theta_7 = 47°$, $\theta_3 = 55°$, $\varphi_3 = 49°$ is only 0.07 kcal/mol below an SAP structure. Several structures which have been described as distorted SAP's are deformed along this coordinate. One interesting system which illustrates this distortion is octacyanotungstate.[6] The d^2 ion in $H_4W(CN)_8 \cdot 6H_2O$[44] or $H_4W(CN)_8 \cdot 4HCl \cdot 12H_2O$[57] is a good approximation to an SAP using the shape parameters of various authors. The d^1 ion in $Na_3W(CN)_8 \cdot 4H_2O$[50] is midway between the SAP and BTP. This is evident from the shape parameters but difficult to see in a drawing.[6]

The number of BTP structures or molecules lying between the SAP and BTP extremes will no doubt increase once the δ, φ shape parameters are fully adopted by structural chemists. Several molecules long identified in the literature as DD or SAP have been reassessed as having BTP geometries.[5,6] For example, the $M(acac)_3 \cdot 2H_2O$ (M = La, Nd, Eu) and the α forms of $M(acac)_4$ (M = Ce, Th) are now recognized[55] as BTP's. Some other examples of this geometry are given in

Table III. Bond Lengths in Some Bicapped Trigonal Prism Structures

compd	M-L_c	M-L_m	M-L_b	ref
ZrF_8^{4-}	2.15[a]	1.91, 1.95	2.20, 2.19	58
$TbCl_3$	2.95	2.70	2.79	59
YF_3	2.25, 2.26	2.27	2.32, 2.30	54
$Eu(acac)_3 \cdot 3H_2O$	2.46 (acac) 2.55 (H_2O)	2.45 2.58	2.49, 2.36, 2.40	60
$La(acac)_3 \cdot 3H_2O$	2.48 (acac) 2.56 (H_2O)	2.49 2.58	2.48, 2.43, 2.47, 2.50	61
$Nd(acac)_3 \cdot 3H_2O$	2.48 (acac) 2.56 (H_2O)	2.44 2.52	2.40, 2.49, 2.38, 2.46	62
α-Nd_2S_3	3.06	2.81	2.97	63
Li_4UF_8	2.39	2.21, 2.24	2.29, 2.26	64
La_2GeS_5	3.03, 2.83	2.86, 2.98	3.15, 2.91, 3.02, 2.96	65
$La_4Ge_3S_{12}$	3.53, 3.00	2.91, 2.98	3.09, 3.02, 2.93, 2.86	66
$Er_8O(dpm)_{10}(OH)_{12}$	2.43	2.34	2.32	67

[a] Involved in hydrogen bonding with hydrazine.

Table III. We note that all of these systems have the d^0 electronic configuration which was indicated as particularly favoring this geometry.

The charge distribution in the BTP is a function of the geometry. For the minimum energy ML_8 conformation, d^2, the population analysis is given in **27**. For the d^0 case the

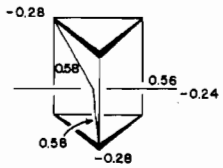

27

overlap populations are slightly larger, but the capping ligands are still the weakest bound. Table III shows some bond lengths in BTP structures. The site notation was defined in **3**. A general lengthening of the metal-to-capping ligand bonds over the others is observed, as we would predict from **27**. The sizable number of different bond lengths in the same molecule testifies to the distorted nature of many of these structures.

The BTP structure is an obvious halfway house between the seven-coordinate capped trigonal prism and the nine-coordinate tricapped trigonal prism. In Li_4UF_8 the U is coordinated to the two capping ligands with U–F bond lengths of 2.39 Å. There is a third F atom just in the right position for coordination to the third face of the prism, 3.3 Å away. In $LiUF_5$ the tricapped structure is found.[58]

Perturbation Theory or Angular Overlap Approach to Eight-Coordination

In this section we focus attention on the forces of interaction between the central metal atom s, p, and d orbitals and the ligand σ orbitals, in an effort to separate electronic effects from steric ones. Our approach will be similar to the one we have used previously in assessing main-group stereochemistry.[69]

Perturbation theory tells us that the stabilization of an orbital i associated with the interaction of two orbitals i and j is given by (1) where the only nonvanishing terms occur in

$$\epsilon_i - \epsilon_i^{(0)} = \epsilon_i^{(2)} + \epsilon_i^{(4)} + \ldots \quad (1)$$

even orders of the perturbation. More specifically we may write (2). The perturbation V_{ij} is $H_{ij} - S_{ij}\epsilon_i^{(0)}$ and an ex-

$$\epsilon_i - \epsilon_i^{(0)} = \frac{|\langle i|V|j\rangle|^2}{\Delta\epsilon_{ij}} - \frac{\epsilon_i^{(2)}|\langle i|V|j\rangle|^2}{(\Delta\epsilon_{ij})^3} + \ldots \quad (2)$$

pression exactly analogous to (2) may be generated by expansion of the secular determinant in a binomial series.[70] If the Wolfsberg–Helmholz approximation for H_{ij} is made, $H_{ij} = {}^1/_2K(H_{ii} + H_{jj})S_{ij}$, and if one further puts $K = 2$, then (2) reduces to the particularly simple form

$$\epsilon_i - \epsilon_i^{(0)} = \frac{H_{jj}^2 S_{ij}^2}{\Delta\epsilon_{ij}} - \frac{H_{jj}^4 S_{ij}^4}{(\Delta\epsilon_{ij})^3} + \ldots \quad (3)$$

This represents an overall stabilization if i is the lower energy one of the two orbitals. For a fixed metal–ligand distance we may express the overlap integral as a simple geometric function of the spherical polar angles defining the ligand positions:

$$S_{ij} = S_\sigma f_{ij}(\theta, \varphi) \quad (4)$$

Expressions for $f_{ij}(\theta, \varphi)$ in terms of trigonometrical functions of these angles are readily available.[71] Amalgamation of (3) and (4) allows us to write the stabilization energy of a ligand σ orbital, i, on interaction with a metal d orbital, j, as in (5).

$$\epsilon_i - \epsilon_i^{(0)} = \beta_\sigma S_\sigma^2 (f_{ij}^2(\theta, \varphi)) - \gamma_\sigma S_\sigma^4 (f_{ij}^4(\theta, \varphi)) \quad (5)$$

Two parameters appear[70] in eq 5: $\beta_\sigma S_\sigma^2 = S_\sigma^2 H_{jj}^2/\Delta\epsilon_{ij}$ and $\gamma_\sigma S_\sigma^4 = S_\sigma^4 H_{jj}^4/(\Delta\epsilon_{ij})^3$. For the case where we have more than a single ligand the stabilization energy of an entire set of eight ligand orbitals (transforming as Γ) on interaction with a central metal orbital is then

$$\Delta\epsilon(\Gamma) = \beta_\sigma S_\sigma^2 \sum_{k=1}^{8} f_{kj}^2(\theta, \varphi) - \gamma_\sigma S_\sigma^4 [\sum_{k=1}^{8} f_{kj}^2(\theta, \varphi)]^2 \quad (6)$$

We are interested in the total σ stabilization afforded the system with two electrons in each ligand-centered orbital. This is simply given by the summation of (6) over all the d orbitals (or over all the p orbitals if we are concerned with those), $\sum(\sigma)$:

$$\sum(\sigma) = 2\sum_{j=1}^{5} [\beta_\sigma S_\sigma^2 \sum_{k=1}^{8} f_{kj}^2(\theta, \varphi) - \gamma_\sigma S_\sigma^4 [\sum_{k=1}^{8} f_{kj}^2(\theta, \varphi)]^2] \quad (7)$$

For the first double summation a simplifying sum rule applies[72]

$$\sum_{j=1}^{5}\sum_{k=1}^{8} f_{kj}^2(\theta, \varphi) = 8 \text{ (number of } \sigma \text{ ligands)} \quad (8)$$

for the d-orbital case, or a similar summation ($j = 1$–3) for p-orbital interaction. Thus the total σ stabilization energy is given by (9), where $h(\theta, \varphi)$ carries the only geometry de-

$$\sum(\sigma) = 16\beta_\sigma S_\sigma^2 - \gamma_\sigma S_\sigma^4 h(\theta, \varphi) \quad (9)$$

pendence of the σ stabilization energy. Note that this result applies specifically to the d^0 configuration. For d^n systems where the d orbitals are partially occupied the sum rule does not usually hold and the geometric preferences of the ligands is most often set by variations in the second-order term of eq 5.[70,73]

Let us apply the results of this discussion to the eight-coordination problem. Three different cases apply. In case 1 there is but a single σ representation to interact with a given d orbital of the same symmetry species. There is in addition only one d orbital (or one set of d orbitals if degenerate) of this particular species. The situation is described exactly by the algebra above. Table I, which listed the irreducible representations subduced by the metal functions and ligand σ orbitals, indicates that this state of affairs is found for three eight-coordinate structures, the **C**, the SAP, and the SP. Figure 5a shows the specific example of the cube. The a_{1g}, a_{2u}, and t_{1u} ligand sets remain σ nonbonding to the metal d manifold (a_{1g} and t_{1u} will interact with s and p orbitals). The stabilization energy of the t_{2g} set is determined by the value of $n_{t_{2g}}$ which is simply the geometrically determined factor given by (10). Values for n for the various geometries are given in Table IV.

$$n_j = \sum_{i=1}^{8} f_{ij}^2(\theta, \varphi) \quad (10)$$

Table IV. n_j Values for Metal–Ligand σ Interactions[a]

		with d orbitals		with p orbitals
DD	a_1	$(3H_A^2 - 1)^2 + (3H_B^2 - 1)^2$	b_2	$4H_A^2 + 4H_B^2$
	b_1	0	e	$2Q_A^2 + 2Q_B^2$
	b_2	$3Q_A^4 + 3Q_B^4$		
	e	$6Q_A^2H_A^2 + 6Q_B^2H_B^2$		
SAP	a_1	$2(3H^2 - 1)^2$	b_2	$8H^2$
	e_2	$3Q^4$	e_1	$4Q^2$
	e_3	$12H^2Q^2$		
SP	a_{1g}	$2(3H^2 - 1)^2$	a_{2u}	$8H^2$
	b_{1g}	$6Q^4$	e_u	$4Q^2$
	b_{2g}	0		
	e_g	$12Q^2H^2$		
C	e_g	0	t_{1u}	$^8/_3$
	t_{2g}	$^8/_3$		
HB	a_{1g}	$^7/_2\ (2 + {}^3/_2)$	a_{2u}	2
	e_{2g}	$^9/_4$	e_{1u}	3
	e_{1g}	0		
BTAP	a_{1g}	$^3/_2(3H^2 - 1)^2 + 2$	a_{2u}	$6H^2 + 2$
	e_g	$3 - {}^3/_4(3H^2 - 1)^2$	e_u	$3Q^2$
	e_g	0		
ETP	a_1'	$^3/_2(3H^2 - 1)^2 + 2$	a_2''	$6H^2 + 2$
	e′	$^9/_4Q^4$	e′	$3Q^2$
	e″	$9Q^2H^2$		
BTP	$a_1(z^2)^b$	$(3H_1^2 - 1)^2 + {}^1/_2(3H_7^2 - 1)^2 + {}^1/_2(3H_5^2 - 1)^2$	a_1	$4H_1^2 + 2H_7^2 + 2H_5^2$
	$a_1(x^2 - y^2)^b$	$3(S^2 - C^2)^2Q_1^4 + {}^3/_4Q_7^4 + {}^3/_4Q_5^4$	b_1	$4Q_1^2S^2 + 2Q_7^2$
	a_2	$12Q_1^4C^2S^2$	b_2	$4Q_1^2C^2 + 2Q_5^2$
	b_1	$6H_7^2Q_7^2 + 12H_1^2Q_1^2S^2$		
	b_2	$6H_5^2Q_5^2 + 12H_1^2Q_1^2C^2$		
PB	a_1'	$^{13}/_4\ (2 + {}^5/_4)$	a_1	2
	e_2'	$^{15}/_8$	e_1	$^5/_2$
	e_1''	0		
TB	a_1'	$^{11}/_4\ (2 + {}^3/_4)$	a_2''	2
	e′	$^9/_8$	e′	$^3/_2$
	e″	0		

[a] $C = \cos\varphi_3$, $S = \sin\varphi_3$, $H = \cos\theta$, $Q = \sin\theta$. [b] The values of n_{a_1} and $n_{a_1'}$ (see Figure 5) are evaluated by solution of a secular determinant where the diagonal elements are those given here and the off-diagonal term is m_{a_1}: $m_{a_1} = 3^{1/2}[2(3H_1^2 - 1)(S^2 - C^2)Q_1^2 - Q_7^2(3H_7^2 - 1) + Q_5^2(3H_5^2 - 1)]$.

For case 2 there are two different types of ligands (DD, HB, BTAP, ETP) and there are always two totally symmetric ligand σ combinations. In the absence of ligand–ligand interactions the result of metal–ligand bonding is that one a_{1g} level remains unchanged in energy and all the latent a_{1g} interaction is "transmitted" to the other. As an example, we use the HB structure in Figure 5b. A similar result applies to the three e_g orbitals in the BTAP, two derived from the d manifold and one from the ligand σ set. One d-orbital combination remains nonbonding and one is antibonding between metal and ligand. The ligand combination is metal–ligand bonding.

Case 3 applies to the C_{2v} BTP structure only. This geometry is of sufficiently low symmetry that two things happen. First, two d orbitals transform as the same irreducible representation of the group and, second, there are now three different types of ligand and consequently three a_1 ligand σ combinations. The result is that an off-diagonal element needs to be introduced into the d orbital–ligand σ problem, of the form

$$m_j = \sum_{i=1}^{8} (f_{ij}(\theta, \varphi))(f_{ik}(\theta, \varphi)) \qquad (11)$$

and a secular determinant solved[74] with diagonal elements of the form of eq 10. The result is an a_1 stabilization for two of the ligand σ combinations of the form $(n_{a_1} \pm n_{a_1}')^2\beta_\sigma S_\sigma^2 - (n_{a_1} \pm n_{a_1}')^4\gamma_\sigma S_\sigma^4$ and zero for the third. Case 3 is shown in Figure 5c.

We may perform an identical treatment for interaction with the $(n + 1)$ p orbitals on the metal. Case 1 or case 2 behavior holds for all systems, in the C_{2v} instance two a_1 ligand σ orbitals receiving zero stabilization. Table IV includes n_j values for these interactions. Overlap of ligand σ orbitals with $(n + 1)$s is isotropic and therefore has no geometrical consequences. We have included the mixing induced by the presence of two d orbitals of the same symmetry, as discussed above. What we will neglect in our treatment is a similar mixing between p and d orbitals (in the DD, ETP, and BTP only) and between s and d orbitals (in all geometries except the C). We shall assume that the total stabilization energy is just the sum of the relevant contributions from s, p, and d interactions.

Since the quartic term from eq 9 comes in with a negative sign, we need to find the minimum value of $h(\theta, \varphi)$ in order to locate the structure of lowest energy. The results for p-orbital interactions alone and d-orbital interactions alone are given in Table V. In many cases the minimum values of θ may be simply derived algebraically from the entries in Table IV.

Some interesting points emerge from Table V. First recall that the extended Hückel calculations arrived at similar geometries within a given distortion coordinate for ML_8 and L_8^{8-}. The table shows, however, that in some cases, for instance, the BTAP and BTP, p, d, and L_8^{8-} (steric) considerations all favor the same geometry. In other cases, for example, the SP, steric, and p-orbital interactions favor one geometry ($\theta = 54.73°$, at the cube) while d-orbital interactions prefer a significantly different structure. In some cases steric, p, and d considerations all prefer different geometries (e.g., the SAP). *However, whatever the desires of p and d electronic*

Table V. Geometry Containing Minimum Value for $h(\theta, \varphi)$

	p	d	minimum L_8^{8-} geometry
DD	a line drawn from the C(θ_A, $\theta_B = 54.73°$) and passing through the points $\theta_A = 42°$, $\theta_B = 70°$ and $\theta_A = 37°$, $\theta_B = 80°$	$\theta_A = 28°$, $\theta_B = 65°$	$\theta_A = 37°$ $\theta_B = 72°$
SAP	$\theta = 54.73°$ ($\cos^2\theta = 1/3$)	$\theta = 66°$	$\theta = 57.5°$
SP	$\theta = 54.73°$ (C) ($\cos^2\theta = 1/3$)	$\theta = 36°$	$\theta = 54.8°$ (C)
BTAP	$\theta = 70.5°$ (C) ($\cos\theta = 1/3$)	($\cos^{-1} 1/3$) $\theta = 70.5°$ (C) ($\cos^{-1}(5^{1/2}/3)$) $\theta = 42°$	$\theta = 70.5°$ (C)
ETP	$\theta = 70.5°$ (C) ($\cos\theta = 1/3$)	$\theta = 60°$	$\theta = 60°$
BTP	a variety of structures, but some around $\theta_1 = 65°$, $\theta_7 = 30°$, $\theta_5 = 65°$, $\varphi_3 = 55°$	a variety of structures, but some around $\theta_1 = 50°$, $\theta_7 = 20°$, $\theta_5 = 65°$, $\varphi_3 = 50°$	$\theta_1 \approx 55°$ $\theta_7 \approx 35°$ $\theta_5 \approx 65°$ $\varphi_3 \approx 49°$

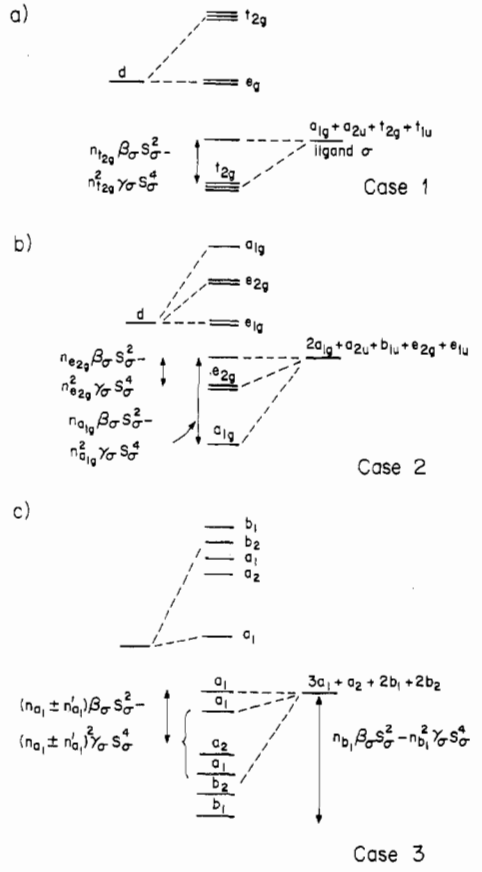

Figure 5. Three different cases of metal–ligand interaction which need to be considered in the perturbation approach. See text for discussion.

interactions, the equilibrium geometry is nearer the sterically determined one than any other.

Table VI shows the values of $h(\theta, \varphi)$ from eq 10 calculated not at the minimum energy p or d geometry from Table V but at the geometry demanded by steric interactions. Included also are the relative energies of the L_8^{8-} molecules at these geometries. Examination of the last two columns gives us a clue as to the reasons for the stability or instability of the various structures. Keep in mind that the summed $h(\theta, \varphi)$ values are not in any energy units, so that only trends can be discerned. Also we simply add d and p contributions together with equal weights. It is clear that the actual situation will be represented by some unequal weighting of the d and p contributions, but we do not know how to choose this.

Table VI. $h(\theta, \varphi)$ Values Evaluated at the Minimum-Energy Geometry for L_8^{8-}

	p orbital	d orbital	sum	energy of L_8^{8-}, kcal/mol
DD	42.6	34.6	77.2	3.5
SAP	43.2	33.2	76.4	0
SP (C)	42.6	42.6	85.2	27
HB[a]	44.0	42.8	86.8	97
ETP	44.8	26.6	71.4	166
BTP	42.6	32.6	75.2	24

[a] This is not the minimum in the BTAP coordinate but is included here since there are a substantial number of structures with this geometry.

As far as steric repulsions are concerned, the systems fall into three groups with increasingly high energy: SAP ~ DD < C ~ BTP ≪ ETP. From electronic considerations we find ETP < BTP < SAP < DD ≪ C ~ HB. The superposition of these two series then gives a good description of the popularity (and thus relative stability) of the various structures. SAP wins out over DD on both counts, but only marginally. These structures are good on both electronic and steric grounds. The BTP is not as happy sterically, but makes up for this on the electronic side. These are the three structures that are most often found. The cube and HB are not very good on either a steric or an electronic basis. As we noted above, there are only a couple of examples of the former, and the HB is especially well stabilized by π interactions which we have neglected here, at least so far. The ETP is a combination of two extremes. While it is predicted to be an excellent structure on electronic grounds, it is exceedingly unstable on steric grounds. The steric effect wins out, for there are no genuine examples of this coordination geometry. We would encourage synthetic efforts to realize this structure by using polydentate or encapsulating ligands which remove some of the steric prohibition. Some studies of six-coordinate trigonal-prismatic geometry have used such ligands,[75a] but here the internuclear distances between metal and capping ligands are large; the structures are essentially six-coordinate.[75b] In **28** the ligand is so designed that the metal–capping ligand distances are not necessarily long. This is the geometrical arrangement in the "football" ligand, for example.[22b]

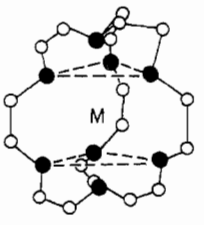

28

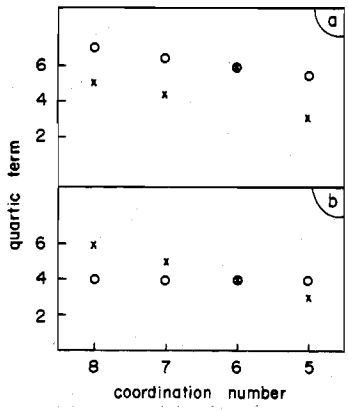

Figure 6. Sizes of the axial (circles) and equatorial (crosses) quartic terms for eight- (HB), seven- (PB), six- (octahedral), and five-coordination (PB) structures: (a) d-orbital interactions; (b) p-orbital interactions. The sizes of the quartic terms, per ligand, are given by $4 + (n/2)$ [axial site, d-orbital interaction], $1 + (11n/6)$ [equatorial, d], 4 [axial, p], and n [equatorial, p], where n is the number of equatorial ligands.

For systems with distinguishable sites (for example, A and B in the DD; axial or equatorial in the HB) we may use this analysis to probe the origins of the differentiation of bond strengths. We extend our analysis to include d^0 examples from five- and seven-coordination in the form of the trigonal bipyramid (TB) and pentagonal bipyramid (PB). The n_j values of eq 10 may be factored into contributions from the two sets of ligands:

$$n_j = n_j(1) + n_j(2) \tag{12}$$

The quartic destabilization energy may be partitoned between the ligands as

$$n_j^2(1) + n_j(1)n_j(2) \text{ and } n_j^2(2) + n_j(1)n_j(2) \tag{13}$$

In Table IV for the HB, PB, and TB structures we have shown the division of n_j in parentheses. For the DD structure the separation is clear from the A,B labels. Figure 6 shows the division of the quartic terms between the axial and equatorial sites, per ligand, for ligand σ–metal p and ligand σ–metal d interactions.

From ligand σ–metal d orbital interactions the axial bonds should always be weaker in TB, PB, and HB (larger quartic term). The bonds are equivalent in the octahedron, by symmetry. On p-orbital grounds the axial bonds should be weaker for the TB and stronger for the PB and HB. Extended Hückel calculations for ML_5, ML_7, and ML_8 with s, p, or d basis sets on the metal bear out this trend (**29**). The relative

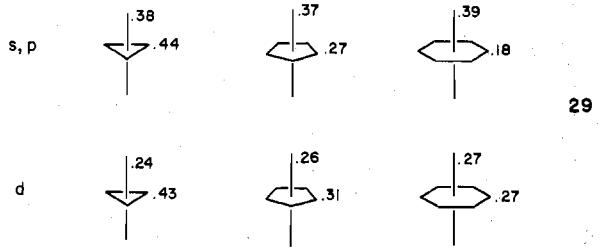

29

bond overlap populations for axial and equatorial groups are dominated by the contribution from metal s,p–ligand σ interaction to give a calculated order of ax < eq (TB); ax > eq (PB, HB). An interesting feature is that the axial overlap populations remain approximately constant in the series TB, PB, and HB, but the equatorial ones steadily decrease in this order. This is a reflection of the fact that the axial three-center bonding constantly uses one metal p orbital, while the equatorial bonding must make do with two p orbitals for an increasing number of bonds. Note that the overlap populations for the HB in **29** do not agree in detail with the full s,p,d basis results given earlier in **8**—additivity is not expected.

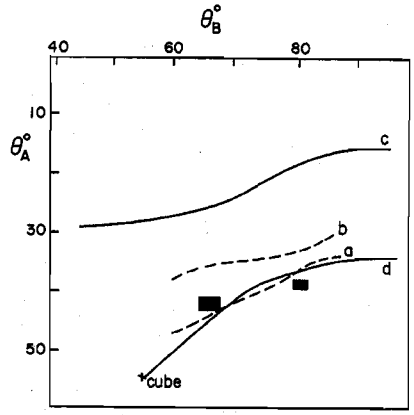

Figure 7. Calculated loci for [bond overlap population (M–A)]/[bond overlap population (M–B)] = 1 for ML_8 (a) and MCl_8 (b) from EHMO calculations and [stabilization energy (M–A)]/[stabilization energy (M–B)] = 1 for ML_8 with d orbitals alone (c) and p orbitals alone (d) from the AOM. The blocks indicate the observed experimental crossover points.

A similar p orbital dominated effect appears to occur in the dodecahedral case. Recall that for some geometries $r_A/r_B < 1$, but for the majority of observed structures $r_A/r_B > 1$. From the relative sizes of the quartic terms for the A and B sites we may construct a picture similar to Figure 4, which is shown in Figure 7. There we see the calculated locus of points where the ratio of A and B overlap populations is equal to unity, as a function of θ_A, θ_B, for our two models using d orbitals alone and p orbitals alone. The results of using extended Hückel calculations for ML_8 and MCl_8 are also shown in the figure. The experimentally observed points where the crossover between $r_A/r_B < 1$ and $r_A/r_B > 1$ are shown as blocks.

While the actual position of the solid lines is not too significant—ligand–ligand interactions are explicitly ignored here but are included in the extended Hückel calculations—it is interesting to see that such a crossover stems from differential electronic stabilization effects, the general form of which may be roughly estimated as a function of θ_A, θ_B. Another interesting point is this: We noticed earlier that above one of the dashed lines of Figure 7 on increasing θ_A the M–A overlap population increased while that of M–B decreased. Below this line they both decreased with increasing θ_A. This is precisely what is seen in the variations of the quartic contributions assigned to A and B ligands from metal d–ligand σ interactions. Slightly more complex behavior is observed with the metal p–ligand σ quartic contributions. Above the crossover line the trend is similar to that of the d-orbital contribution. An increase in the quartic terms for both A and B on increasing θ does not occur until larger values of θ_A, rather than at the crossover line.

π Bonding in DD and SAP Structures

It is clear now that these two geometries are close in energy. We have considered some of the factors that may favor one relative to another. At this point we proceed to discuss how π bonding may influence the two structures. This is an area where many authors have made contributions initiated by an early and important comment by Orgel.[10e]

In the DD the lowest lying d orbital is the σ-nonbonding $x^2 - y^2$. The overlap integral of a ligand $\pi_\perp$ orbital with this $x^2 - y^2$ orbital (**30**) is given by the function $S(\theta) = S_\pi \sin \theta$. Using the angular overlap approach the interaction energy to second order is $\beta_\pi S_\pi^2 \sin^2 \theta$. (We note here an earlier AOM treatment of this problem.[35]) Thus the largest interaction will be for the ligands with the largest value of θ, i.e., the B ligands. If this interaction leads to an overall electronic stabilization

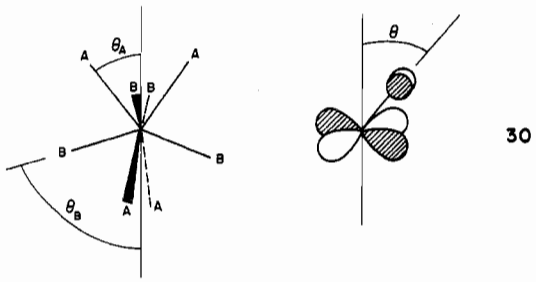

30

(d^2 with a π acceptor, **31**, or d^0 with a π donor, **32**), then the π-bonding ligands should enter the B sites. If the overall effect is a four-electron destabilizing one (d^2 with a π donor, **33**), then the donors should prefer the A sites.

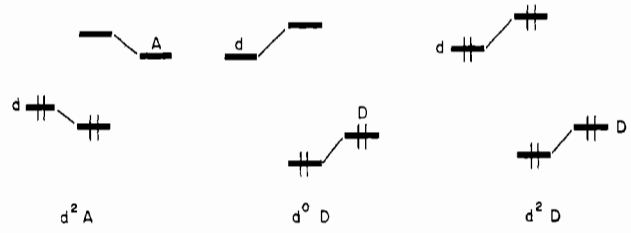

31 32 33

This is the basis of Orgel's rule. Its corollary is that in any $ML_4L'_4$ complex the L and L′ ligands should sort themselves into the A and B sites such that all the sites of one kind are occupied only by ligands of one kind. One piece of evidence cited which supports this π-interaction determinant of stereochemistry appeared in Table II. There is an inversion in site preferences in the $M(quin)_4$ molecules depending on the number of d electrons (M = W, d^2; = Zr, d^0). The conclusion here is that the O atoms are π donors, avoiding the B sites in the d^2 system, and the N atoms relative to these are π acceptors. However, the chelation mode changes as well on changing the number of d electrons. In the Zr system it is the *g* edges which are chelated and in the W analogue it is the *m* edges. No inversion of ligand site preference is seen[31,32] in the halfway d^1 structures $V(Nb)Cl_4(diars)_2$ compared to d^0 $TiCl_4(diars)_2$. It is argued that the RNC ligand is a better π acceptor than CN and that Orgel's rule also applies[36] for $Mo(CN)_4(RNC)_4$ where the RNC occupies the B sites. However, we also saw that for most of these structures it was the more electronegative ligand which occupied the B sites, in agreement with the σ site preference conclusion which we reached earlier. We think that the site preferences in the DD are very likely determined by a combination of σ, π, and steric (e.g., $H_4Mo(PPh_3)_4$) effects.

$\pi_{\parallel}$ orbitals have no overlap with $x^2 - y^2$. Thus any single-faced π ligand should orient itself in the $\perp$ orientation for cases **31** and **32** and in the $\parallel$ orientation for **33**. acac and related chelate systems which are π donors should then prefer to chelate via use of the *m* edges for d^0 structures since here the π effect is maximized without chelate distortion. For d^1 or d^2 structures we might expect to find other chelation modes which relieve the destabilization. However, the *mmmm* isomer is an excellent choice on steric grounds[8] and there seems to be no dramatic shift in the mode of isomer chelation with d electron count. Thus $V^{IV}(dtb)_4$,[76a,b] $W^{IV}(quinBr)_4$,[35] $Ti^{IV}(dtc)_4$,[76c] and $Zr^{IV}(NO_3)_2(acac)_2$[42] all follow the *mmmm* chelation pattern. The electronic configurations of this series are d^1, d^2, d^0, and d^0, respectively. $Zr^{IV}(NO_3)(acac)_3$ (d^0), however, has the unusual *abmg* pattern[77] and the $V^{IV}(dta)_4$ crystal structure contains two symmetry-unrelated molecules, one with *mmmm* and the other with the rare *mmgg* chelation.[78]

For the SAP the lowest energy d orbital is z^2 and π bonding may occur in the fashion illustrated in **34**. The angular

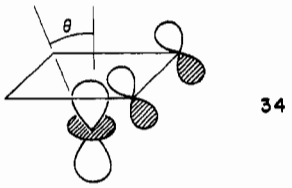

34

dependence of overlap here is given by the function $S = 3^{1/2} \cdot \sin\theta \cos\theta$, and thus the stabilization energy is $3S_\pi^2 \sin^2\theta \cos^2\theta$. This has a maximum at $\theta = 45°$. By comparing the total π-type interaction energies for SAP ($\theta = 58°$) and DD ($\theta_A = 36°$, $\theta_B = 74°$) we find a larger interaction, by 5%, for the DD relative to SAP.

Although it is hazardous to attach too much quantitative weight to what follows, let us try to delineate those factors which may stabilize one structure relative to the other. For d^1, d^2 systems DD is favored over SAP on σ grounds (recall the lowest d orbital is strictly σ nonbonding in DD but slightly antibonding in SAP) and also favored on π-bonding grounds for systems with π-acceptor ligands. For the d^0 case the SAP seems to be favored, very slightly, over DD on electronic σ and steric grounds, but the DD receives more π stabilization from π donors. The unraveling of the relative importance of all these effects is obviously not possible at present, especially since the experimental evidence is also perturbed by differential solvation effects in solution and crystal packing forces in the solid.

We note here the Kepert result,[7b] that the DD structure is preferred over SAP for small-bite ligands, does seem to be borne out for many species. O_2^{2-}, mono- and dithiocarbamates, and NO_3^- invariably give DD structures. The structure of $Ce(IO_3)_4 \cdot H_2O$ is a SAP, but here the Ce atom is coordinated[79] to only one of the O atoms of a particular IO_3^- unit.

One particularly interesting effect occurs in the SAP structures with coordinated acac ligands. This is the folding of the acac–metal ring around the O···O axis, **35**, for in-

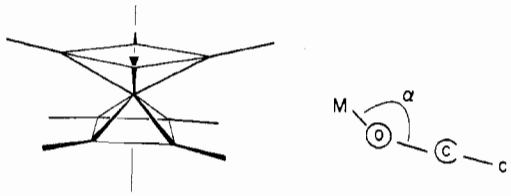

35

stance,[80,81] in $M^{IV}(acac)_4$, M = Zr, Ce, U, where the *ssss* isomer is found. This leaves the acac still planar but tilted. The angle α is typically around 160°. Folding at acac rings in other systems which are not eight-coordinate also occurs, for instance, in $VO(acac)_2$,[82] $Co(acac)_2(H_2O)_2$,[83] and $Zn(acac)_2(H_2O)$,[84] but not in $Zn(dpm)_2$[85] and only to a very small extent in SAP structures coordinated in *llll* fashion,[86] e.g., $Th^{IV}(tfac)_4$ and $Nb^{IV}(dpm)_4$. Our calculations indicate that the folding in some of these structures is a low-energy process and certainly will occur in the crystal if it is required to aid molecular packing.

The rather larger folding found in the $M^{IV}(acac)_4$ systems where the coordination is *ssss* has a molecular orbital rationale that may also be important. The detailed molecular orbital argument is a complex one, but the stabilization on bending for the $Zr(acac)_4$ structure may be traced to a metal–ligand bonding orbital involving among other things these π-donor orbitals on the ligands. As the ligand is folded around the O···O axis, the π orbital is tilted to interact in a better fashion with z^2. A part of the extra stabilization energy arises from the folding downward of the ligand to increase π bonding. For *llll* coordinated ligands there is little advantage to be gained by ligand folding and the angles observed here are small.

Table VII. Site Preference Guide

	Dodecahedron
d^2 A and d^0 D	$\perp_B > \perp_A > \parallel_A \sim \parallel_B$
d^2 D	$\parallel_A \sim \parallel_B > \perp_A > \perp_B$
	Square Antiprism
d^2 A and d^0 D	$\parallel > \perp$
d^2 D	$\perp > \parallel$
	Bicapped Trigonal Prism
d^2 A and d^0 D	$(m_\parallel \sim b_\parallel) > b_\perp > (c_\parallel \sim c_\perp \sim m_\perp)$
d^2 D	$(m_\perp \sim c_\perp \sim c_\parallel) > b_\perp > (b_\parallel \sim m_\parallel)$
	Hexagonal Bipyramid
d^2 A and d^0 D	$eq_\parallel \sim ax > eq_\perp$
d^2 D	$eq_\perp > eq_\parallel \sim ax$

Similar ligand folding is also not expected in *mmmm* chelated DD structures since maximum π overlap is achieved without folding.

Site Preferences of π Donors and Acceptors

As in the analysis of the seven-coordinate structural problem, we use a combination of test orbitals and Cl and CO substituents to probe the site preferences and orientations of ligand-bearing π orbitals. We saw in the previous section for DD and SAP structures that there was no interaction of $\pi_\parallel$ orbitals with the lowest energy d orbital in the DD and no interaction of $\pi_\perp$ orbitals with the lowest energy d orbital in the SAP geometry. The site and orientation preferences for donor (D) and acceptor (A) π ligands in these and other structures are summarized in a site preference guide, Table VII.

For the HB or BTAP structure there is a low-lying pair of d orbitals available for interaction with both axial and $eq_\parallel$ π orbitals, **36** and **37**. $Eq_\perp$ π orbitals are of the wrong symmetry

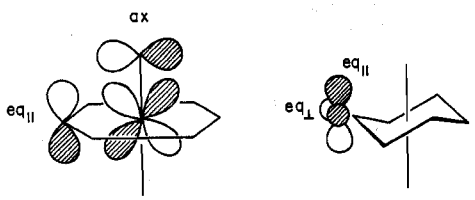

36 **37**

to interact with this low-energy pair. We note here that both π orbitals on an axial ligand may interact optimally with the central atom *xz*, *yz* pair. This is the only structure among those we consider where this is so. From our analysis of σ effects above, the axial sites in d^0 complexes are then very strongly bound by a powerful combination of σ- and π-bonding effects. There are many HB complexes based on the linear UO_2 unit to underline this point.

For the BTP the lowest lying d orbital is a combination of z^2 and $x^2 - y^2$. Two views are shown in **38** and **39**. The three

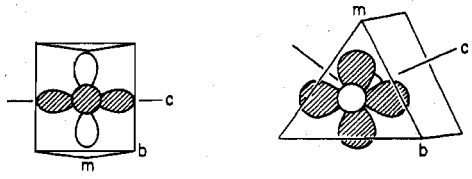

38 **39**

possible types of π-substituent orientations appear in **40**. The $c_\perp$ and $m_\perp$ have no interaction with this orbital at all. $c_\parallel$ has a small interaction with the z^2 component. This may be related to the $\pi_\parallel$–z^2 overlap of the SAP, with the large value of θ responsible for the poor overlap. $b_\parallel$ and $m_\parallel$ have a good interaction with z^2. $b_\perp$ may interact with the $x^2 - y^2$ component of this orbital. The site preference guide for this

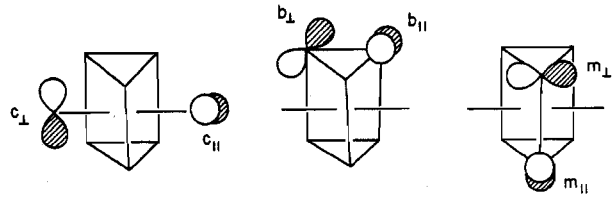

40

geometry also appears in Table VII. We note the general superiority of $\parallel$ interactions over $\perp$ ones—a reminder of the SAP parentage of this structure. For cylindrically symmetrical π systems the largest interaction is in the m or b positions. The experimental data available on molecules with BTP geometry are not at present good enough to test out these ideas. In addition, as we saw with the DD structure, all effects—steric, σ, and π—may enter into determination of the substituent arrangement.

Complexes with More Than Two d Electrons

There are several examples of these: $Co(CF_3CO_2)_4^{2-}$,[87] $M(NO_3)_4^{n-}$ [M = Mn(II),[25] Fe(III),[88] Co(II),[89] Zn(II)[90]],[91] and $M(OAc)_4^{2-}$[94] [M = Cu, Cd]. All of these depart significantly from the calculated valley in the θ_A, θ_B potential energy surface of Figure 3. Such distortion may not immediately be ascribed to the presence of more than two d electrons, since CrO_8^{3-}, d^1, also has a distorted structure.[10i] It does, however, seem to be a consequence of the presence of the small-bite ligands NO_3^-, OAc^-, and O_2^{2-}. These molecules show some structural similarities. All are chelated *mmmm*. Values of θ_B (**41**) are fairly constant (80.5–83.7°),

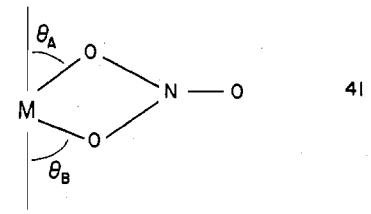

41

but the values of θ_A are sensitive to the d-orbital configuration: Ti(IV) [d^0], 37°; Fe(III) [h.s. d^5], 38.7°; Mn(II) [h.s. d^5], 43.0°; Co(II) [h.s. d^7], 46.5°; Zn(II) [d^{10}], 46.8° for the nitrates and 48.5° for Co(II) [h.s. d^7] in $Co(CF_3CO_2)_4^{2-}$. As θ_A increases, the bonds to the B sites become weakened relative to those to the A sites. For Mn(II), Fe(III), and Zn(II) with spherically symmetrical d configurations, relative bond overlap populations similar to the d^0 case are expected. Thus these points may usefully be plotted on Figure 3. We see the predicted crossover from $r_A/r_B > 1$ to $r_A/r_B < 1$ between the geometries of the isoelectronic Mn(II), Fe(III) systems.

Figure 8 shows the energetic behavior of the metal d orbitals at $\theta_B = 81°$ as θ_A is increased. From the calculations, increasing θ_A is favored in the order h.s. d^5 < h.s. d^7 < d^{10}. The double occupation of z^2 in the h.s. d^7 and d^{10} structures is the driving force to increasing θ_A in this series. Note that a h.s. d^7 system with $\theta_A \lesssim 40$ is Jahn–Teller unstable.

The $Cu(OAc)_4^{2-}$ structure is probably best regarded as derived from a square-planar d^9 complex with long axial bonds, a feature typical of these systems. In this case we have long axial pairs of bonds and an r_A/r_B ratio of 1.41. The analogous Cd(II) species (d^{10}) has a very similar angular geometry, but with a much smaller bond length ratio of 1.17 to emphasize this point.

Polytopal Rearrangements

In this section we discuss briefly the energetics of possible rearrangement pathways between the idealized structural extremes. For the high-energy set of geometries (HB, BTAP, C) the potential energy surface connecting them via **1** is a

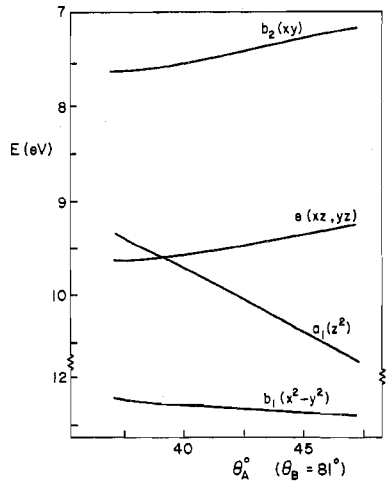

Figure 8. The energies of the metal d orbitals and the DD configuration with $\theta_B = 81°$ and a varying θ_A for the $M(NO_3)_4$ molecule.

smooth one, with a minimum at the cube geometry for all the systems we have studied. These always have eight identical ligands and so exclude the UO_2-type structures in which two ligands selectively take advantage of the special bonding possibilities of the HB. Rearrangement of the HB structure could in principle involve an excursion to the cube and back.

Of more interest are the energetics of rearrangement of the low-energy set of geometries (DD, SAP, BTP). Figure 2 showed several views of the DD structure, one of which emphasizes its relationship to the BTP. In turn **3** showed how the BTP is readily reached from the SAP by conversion of one SAP square face to a diamond face of the BTP. One pathway of interconversion of DD and SAP is therefore via the BTP. Another route was shown in **5**—rotation of the "upper hemisphere" ligands against the "lower hemisphere" ones with simultaneous relaxation of the angles made by the ML bonds with the rotation axis coming out of the plane of the paper. A third route was shown in **6**. This involves simultaneous conversion of the two SAP square faces to diamond faces of the DD and may also be viewed as the rotation of pairs of A and B ligands against each other, **42**, as suggested by Kepert.[7c]

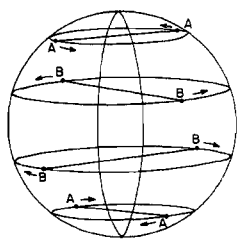

42

For the ML_8 system our calculations indicate that there is no barrier for this motion, the energy profile for both d^0 and d^2 configurations being set purely by the energies of the DD and SAP end points. Basically there are no barriers to geometrical interconversion along at least one pathway, if not several, between DD and SAP. We may get a barrier to interconversion if this pathway is not accessible, if on rearrangement an unfavorable chelation mode is created.

Many of these eight-coordinate systems are fluxional on the NMR time scale. $Mo(CN)_8^{4-}$ shows a single ^{13}C resonance in solution suggesting a rapid interchange of dodecahedral sites by a process which has been shown to be intramolecular.[95] Similarly, $H_5Ir[C_6H_5P(C_2H_5)_2]_3$[96] ($d^4$) and $ReH_5[P(C_6H_5)_3]_3$[97] (d^2) give NMR spectroscopic equivalence of ligand nuclei. Only recently have NMR studies on tetrakis chelates given structural and stereochemical information because of very rapid stereochemical rearrangements.[98,99] For $U(acac)_4$ in a Freon solvent[99] the single time-averaged methyl resonance splits into two below −137 °C. Temperature studies give a value of $\Delta H^\ddagger = 6.0 \pm 0.1$ kcal/mol. For $Zr(acac)_4$ the figure is even lower, 4.1 ± 0.3 kcal/mol. Both rearrangement processes are intramolecular. These low-energy pathways will surely be strongly influenced by the steric properties of the ligands in addition to electronic effects as we have emphasized throughout this paper. Interestingly, stereochemical nonrigidity in these eight-coordinate systems was first demonstrated using H_4ML_4 (M = Mo, W; L = PR_3)[100] where $\Delta G^\ddagger = 12$–16 kcal/mol. Unfortunately, the NMR spin system is complex and the spectra carry so little information that a permutation analysis was not possible.

Table VIII. Extended Hückel Parameters

orbital	H_{ii}	exponents	orbital	H_{ii}	exponents
L 1s	−15.0	1.300	Cl 3s	−30.0	2.033
C 2s	−21.4	1.625	Cl 3p	−15.0	2.033
C 2p	−11.4	1.625	Mo 5s	−10.5	1.630
O 2s	−32.3	2.275	Mo 5p	−5.98	1.550
O 2p	−14.8	2.275	Mo 4d[a]	−14.3	3.610 (0.5211)
					1.610 (0.6358)

[a] Two Slater exponents are listed for the 4d functions. Each is followed in parentheses by the coefficient in the double-ζ expansion.

Acknowledgment. Conversations with E. L. Muetterties and S. J. Lippard were important in providing the impetus for this work. We are grateful to the National Science Foundation for its support of this work through Grants CHE-76-06099 and CHE-76-20300. J.K.B. thanks R.H. for his superb hospitality during his stay at Cornell. We also thank Y.-C. Tse for her assistance with some of the calculations, E. Kronman for the typing, J. Jorgensen for the drawings, and D. L. Kepert for making his work available to us before publication.

Appendix

The method of calculation used is the extended Hückel procedure[101] and the parameters used in our calculations are given in Table VIII. The test metal atom was Mo with a double-ζ 4d function.[102] L is the pseudoligand we have used before which carries a single 1s orbital. Bond distances were M–L = 1.65 Å, M–CO = 1.97 Å, M–Cl = 2.45 Å, and C–O = 1.14 Å. To probe π-donor and -acceptor character 2p test orbitals with exponents of 2.200 were added to the σ ligand L in the correct orientation. The p orbital H_{ii} value and total number of electrons were adjusted to make the p orbitals strong or weak donors or acceptors, as desired.

References and Notes

(1) On leave from the University of Newcastle-upon-Tyne, Newcastle-upon-Tyne, NE1 7RU, England. Present address: Chemistry Department, University of Chicago, Chicago, Ill. 60637.
(2) Reviews on eight-coordination: (a) E. L. Muetterties and C. M. Wright, *Q. Rev., Chem. Soc.*, **21**, 109 (1967); (b) S. J. Lippard, *Prog. Inorg. Chem.*, **8**, 109 (1967); (c) S. J. Lippard, *ibid.*, **21**, 91 (1976); (d) R. V. Parish, *Coord. Chem. Rev.*, 1, 439 (1966); (e) D. L. Kepert, submitted for publication in *Prog. Inorg. Chem.*; (f) R. J. H. Clark, D. L. Kepert, R. S. Nyholm, and J. Lewis, *Nature (London)*, **199**, 559 (1963); (g) M. G. B. Drew, *Coord. Chem. Rev.*, **24**, 179 (1977).
(3) J. Felsche, *Struct. Bonding (Berlin)*, **13**, 99 (1973).
(4) R. A. Penneman, R. R. Ryan, and A. Rosenzweig, *Struct. Bonding (Berlin)*, **13**, 1 (1973).
(5) M. A. Porai-Koshits and L. A. Aslanov, *J. Struct. Chem. (Engl. Transl.)*, **13**, 244 (1972).
(6) E. L. Muetterties and L. J. Guggenberger, *J. Am. Chem. Soc.*, **96**, 1748 (1974).
(7) (a) D. L. Kepert, *J. Chem. Soc.*, 4736 (1965); (b) D. G. Blight and D. L. Kepert, *Inorg. Chem.*, **11**, 1556 (1972); (c) D. G. Blight and D. L. Kepert, *Theor. Chim. Acta*, **11**, 51 (1968).
(8) J. L. Hoard and J. V. Silverton, *Inorg. Chem.*, **2**, 235 (1963).
(9) For other studies using this approach see: (a) R. B. King, *J. Am. Chem. Soc.*, **92**, 6455 (1970); (b) T. W. Melnyk, O. Knop, and W. R. Smith, *Can. J. Chem.*, **55**, 1745 (1977).

(10) (a) R. V. Parish and P. G. Perkins, *J. Chem. Soc. A.*, 345 (1967); (b) A. Golebiewski and H. Kowalski, *Theor. Chim. Acta*, **12**, 293 (1968); (c) G. Racah, *J. Chem. Phys.*, **11**, 214 (1943); (d) G. H. Duffey, *J. Chem. Phys.*, **18**, 746, 1444 (1950); (e) L. E. Orgel, *J. Inorg. Nucl. Chem.*, **14**, 136 (1960); (f) J. R. Perumareddi, A. D. Liehr, and A. W. Adamson, *J. Am. Chem. Soc.*, **85**, 249 (1963); (g) G. Gliemann, *Theor. Chim. Acta*, **1**, 14 (1962); (h) M. Basu and S. Basu, *J. Inorg. Nucl. Chem.*, **30**, 467 (1968); (i) J. D. Swalen and J. A. Ibers, *J. Chem. Phys.*, **37**, 17 (1962); (j) B. R. McGarvey, *Inorg. Chem.*, **5**, 476 (1966); (k) M. Randič, *Croat. Chem. Acta*, **32**, 189 (1960); (l) V. M. Volkov and M. E. Dyatkina, *J. Struct. Chem. (Engl. Transl.)*, **5**, 561 (1964). (m) A discussion of the CrO_8^{3-} system from a different viewpoint is in N. Rösch and R. Hoffmann, *Inorg. Chem.*, **13**, 2656 (1974).

(11) For a discussion of the photochemistry of the octacyanides see Z. Stasicka, *Zesz. Nauk. Uniw. Jagiellan, Pr. Chem.*, **No. 18**, 39 (1973).

(12) A. R. Rossi and R. Hoffmann, *Inorg. Chem.*, **14**, 365 (1975).

(13) R. Hoffmann, B. F. Beier, E. L. Muetterties, and A. R. Rossi, *Inorg. Chem.*, **16**, 511 (1977).

(14) A selective but not exhaustive list of HB geometries: (a) S. Marangoni, S. Degetto, R. Graziani, and G. Bombieri, *J. Inorg. Nucl. Chem.*, **36**, 1787 (1974); (b) J. E. Fleming and H. Lynton, *Chem. Ind. (London)*, 1409 (1959); (c) J. C. Taylor and M. H. Mueller, *Acta Crystallogr.*, **19**, 536 (1965); (d) N. K. Dalley, M. H. Mueller, and S. H. Simonsen, *Inorg. Chem.*, **10**, 323 (1971).

(15) N. Rysanik and O. Loye, *Acta Crystallogr., Sect. B*, **29**, 1567 (1963).

(16) (a) G. Bombieri and K. W. Bagnall, *J. Chem. Soc., Chem. Commun.*, 188 (1975). (b) The reverse site occupancy for $UCl_2(Me_2SO)_6^{2+}$ is given incorrectly by M. B. Hursthouse in *Mol. Struct. Diff. Methods.*, **4** (1976). (c) R. P. Dodge, G. S. Smith, Q. Johnson, and R. E. Elson, *Acta Crstallogr. Sect. B*, **24**, 304 (1968).

(17) (a) R. Countryman, and W. S. McDonald, *J. Inorg. Nucl. Chem.*, **33**, 2213 (1971); (b) G. Bombieri, P. T. Moseley, and D. Brown, *J. Chem. Soc., Dalton Trans.*, 1520 (1975).

(18) D. Brown, J. F. Easey, and C. E. F. Rickard, *J. Chem. Soc. A*, 1161 (1969).

(19) G. Del Piero, G. Perego, A. Zazzetta, and G. Brandi, *Cryst. Struct. Commun.*, **4**, 521 (1975).

(20) W. H. Zachariasen, *Acta Crystallogr.*, **2**, 388 (1949).

(21) (a) M. Dobler, J. D. Dunitz, and B. T. Kilbourn, *Helv. Chim. Acta*, **52**, 2573 (1969); (b) Y. Nawata, T. Sakamaki, and Y. Iitaka, *Acta Crystallogr., Sect. B*, **33**, 1201 (1977).

(22) (a) D. E. Fenton, C. Nave, and M. R. Truter, *J. Chem. Soc., Dalton Trans.*, 2188 (1973); (b) B. Metz, D. Moras, and R. Weiss, *Chem. Commun*, 444 (1971).

(23) T. L. Cottrell, "The Strengths of Chemical Bonds", Butterworths, London, 1958.

(24) (a) J. L. Hoard and H. H. Nordsieck, *J. Am. Chem. Soc.*, **61**, 2853 (1939); (b) J. L. Hoard, T. A. Hamor, and M. D. Glick, *ibid.*, **90**, 3177 (1968).

(25) J. Drummond and J. S. Wood, *J. Chem. Soc. A*, 226 (1970).

(26) W. L. Cox, H. Steinfink, and W. F. Bradley, *Inorg. Chem.*, **5**, 318 (1966).

(27) A. V. Virkar, P. P. Singh, and A. Raman, *Inorg. Chem.*, **9**, 353 (1970).

(28) W. Mark and M. Hansson, *Acta Crystallogr., Sect. B*, **31**, 1101 (1975).

(29) (a) Reference 93; (b) Reference 88; (c) Reference 25; (d) Reference 89; (e) Reference 90; (f) Reference 87; (g) Reference 10i; (h) Reference 94; (i) Actinide fluoride examples from ref 4; (j) Actinide chloride and bromide examples from D. Brown, T. L. Hall, and P. T. Moseley, *J. Chem. Soc., Dalton Trans.*, 686 (1973); (k) Reference 75a; (l) Reference 35; (m) R. C. L. Mooney, *Acta Crystallogr.*, **2**, 189 (1949); (n) H. Bode and G. Teufer, *ibid.*, **9**, 929 (1956); (o) D. F. Lewis and R. C. Fay, *Inorg. Chem.*, **15**, 2219 (1976); (p) Reference 101 in ref 2b; (q) Reference 27; (r) Reference 76; (s) Reference 31; (t) T. C. W. Mak, *Can. J. Chem.*, **46**, 3491 (1968); (u) J. V. Silverton, J. L. Hoard, and G. L. Glenn, *Inorg. Chem.*, **2**, 250 (1963); (v) Reference 78b; (w) Reference 30; (x) Reference 24; (y) Reference 36; (z) Reference 33; (aa) R. A. Lalancette, M. Cefola, W. C. Hamilton, and S. J. La Placa, *Inorg. Chem.*, **6**, 2127 (1967); (bb) M. J. Bennett, F. A. Cotton, P. Legzdins, and S. J. Lippard, *Inorg. Chem.*, **7**, 1770 (1968); (cc) M. G. B. Drew, A. P. Wolters, and J. D. Wilkins, *Acta Crystallogr., Sect. B*, **31**, 324 (1975); (dd) Reference 17.

(30) L. J. Guggenberger, *Inorg. Chem.*, **12**, 2295 (1973).

(31) R. J. H. Clark, J. Lewis, R. S. Nyholm, P. Pauling, and G. B. Robertson, *Nature (London)*, **192**, 222 (1961).

(32) R. J. H. Clark, D. L. Kepert, J. Lewis, and R. S. Nyholm, *J. Chem. Soc.*, 2865 (1965).

(33) D. C. Bradley, M. B. Hursthouse, and I. F. Randall, *Chem. Commun.*, 368 (1970).

(34) D. F. Lewis and R. C. Fay, *J. Chem. Soc., Chem. Commun.*, 1046 (1974).

(35) W. D. Bonds, R. D. Archer, and W. C. Hamilton, *Inorg. Chem.*, **10**, 1764 (1971).

(36) (a) F. H. Cano and D. W. J. Cruickshank, *Chem. Commun.*, 1617 (1971); (b) M. Novotny, D. F. Lewis, and S. J. Lippard, *J. Am. Chem. Soc.*, **94**, 6961 (1972).

(37) A. I. Pozhidaev, M. A. Porai-Koshits, and T. N. Polynova, *J. Struct. Chem. (Engl. Transl.)*, **15**, 548 (1974).

(38) J. L. Hoard, E. Willstadter, and J. V. Silverton, *J. Am. Chem. Soc.*, **87**, 1610 (1965).

(39) C. Ayasse and H. A. Eick, *Inorg. Chem.*, **12**, 1140 (1973).

(40) N. K. Bel'skii and Yu. T. Struchkov, *Sov. Phys.—Crystallogr. (Engl. Transl.)*, **10**, 16 (1965).

(41) (a) W. L. Steffen and R. C. Fay, *Inorg. Chem.*, **17**, 2120 (1978); (b) W. L. Steffen, S. L. Hawthorne, and R. C. Fay, *J. Am. Chem. Soc.*, **98**, 6757 (1976).

(42) V. W. Day and R. C. Fay, *J. Am. Chem. Soc.*, **97**, 5136 (1975).

(43) The crystals are isomorphous with $K_4Mo(CN)_8 \cdot 2H_2O$: see ref. 24a. For a survey of the checkered history of the geometry (especially in solution) of the $M(CN)_8^{3-,4-}$ (M = Mo, W) over the years see ref 24b and 46.

(44) S. S. Basson, L. D. C. Bok, and J. G. Leipoldt, *Acta Crystallogr., Sect. B*, **26**, 1209 (1970).

(45) J. Chojnacki, J. Grochowski, L. Leboida, B. Oleksyn, and K. Stadnicka, *Roczn. Chem.*, **43**, 273 (1969).

(46) R. A. Pribush and R. D. Archer, *Inorg. Chem.*, **13**, 2556 (1974).

(47) W. E. Bennett, D. E. Broberg, and N. C. Baenziger, *Inorg. Chem.*, **12**, 930 (1973).

(48) A. Gieren and W. Hoppe, *Chem. Commun.*, 413 (1971).

(49) J. Iball, J. N. Low, and T. J. R. Weakley, *J. Chem. Soc., Dalton Trans.*, 2021 (1974).

(50) L. D. C. Bok, J. G. Leipoldt, and S. S. Basson, *Acta Crystallogr., Sect., B*, **26**, 684 (1970).

(51) For a comparison of the $Mo(CN)_8$ 4– and 3– structures see: B. J. Corden, J. A. Cunningham, and R. Eisenberg, *Inorg. Chem.*, **9**, 356 (1970).

(52) S. Haddah and P. S. Gentile, *Inorg. Chim. Acta*, **12**, 131 (1975).

(53) A. R. Al-Karaghouli and J. S. Wood, *J. Chem. Soc., Chem. Commun*, 516 (1972).

(54) A. Zalkin and D. H. Templeton, *J. Am. Chem. Soc.*, **75**, 2453 (1953).

(55) W. L. Steffen and R. C. Fay, *Inorg. Chem.*, **17**, 779 (1978); see also ref 56 for a contemporary study without the use of such parameters.

(56) B. Allard, *J. Inorg. Nucl. Chem.*, **38**, 2109 (1976).

(57) L. D. C. Bok, J. G. Leipoldt, and S. S. Basson, *Z. Anorg. Allg. Chem.*, **392**, 303 (1972).

(58) B. Kojic-Prodic, S. Scavinicar, and B. Matkovic, *Acta Crystallogr., Sect. B*, **27**, 638 (1971).

(59) J. D. Forrester, A. Zalkin, D. H. Templeton, and J. C. Wallman, *Inorg. Chem.*, **3**, 185 (1964).

(60) A. L. Il'inskii, L. A. Aslanov, V. I. Ivanov, A. D. Khalilov, and O. M. Petrukhin, *J. Struct. Chem. (Engl. Transl.)*, **10**, 263 (1969).

(61) T. Phillips, II, D. E. Sands, and W. F. Wagner, *Inorg. Chem.*, **7**, 2295 (1968).

(62) L. A. Aslanov, M. A. Porai-Koshits, and M. O. Dekaprilevich, *J. Struct. Chem. (Engl. Transl.)*, **12**, 431 (1971).

(63) A. A. Eliseev, S. J. Uspenskaya, A. A. Fedorov, and M. Tolstova, *J. Struct. Chem. (Engl. Transl.)*, **13**, 66 (1972).

(64) G. Brunton, *J. Inorg. Nucl. Chem.*, **29**, 1631 (1967).

(65) A. Mazurier and J. Etienne, *Acta Crystallogr., Sect. B*, **29**, 817 (1973).

(66) A. Mazurier and J. Etienne, *Acta Crystallogr., Sect. B*, **30**, 759 (1974).

(67) J. C. A. Boeyens and J. P. R. de Villiers, *J. Cryst. Mol. Struct.*, **2**, 197 (1972).

(68) G. Brunton, *Acta Crystallogr.*, **21**, 814 (1966).

(69) J. K. Burdett, *Struct. Bonding (Berlin)*, **31**, 67 (1977).

(70) J. K. Burdett, *Inorg. Chem.*, **14**, 375 (1975).

(71) See, for example, W. Smith and D. W. Clack, *Rev. Roum. Chim.*, **20**, 1252 (1975).

(72) C. E. Schäffer and C. K. Jørgensen, *Mol. Phys.*, **9**, 401 (1964).

(73) J. K. Burdett, *Adv. Inorg. Chem. Radiochem.*, **21**, 113 (1978).

(74) (a) M. Gerloch and R. C. Slade, "Ligand Field Parameters", Cambridge University Press, New York, N.Y., 1973, p 178; (b) D. S. McClure in "Advances in the Chemistry of the Coordination Compounds", S. Kirschner, Ed., Macmillan, New York, N.Y., 1961, p 501.

(75) (a) E. Larsen, G. N. La Mar, B. E. Wagner, J. E. Parks, and R. H. Holm, *Inorg. Chem.*, **11**, 2652 (1972); (b) M. R. Churchill and A. H. Reis, *Inorg. Chem.*, **11**, 1811 (1972).

(76) (a) M. Bonamico, G. Dessy, V. Fares, P. Porta, and L. Scaramuzza, *Chem. Commun.*, 365 (1971); (b) M. Bonamico, G. Dessy, V. Fares, and L. Scaramuzza, *Cryst. Struct. Commun.*, **1**, 91 (1972); (c) M. Colapietro, A. Vaciago, D. C. Bradley, M. B. Hursthouse, and I. F. Rendall, *J. Chem. Soc., Dalton Trans.*, 1052 (1972).

(77) E. G. Muller, V. W. Day, and R. C. Fay, *J. Am. Chem. Soc.*, **98**, 2165 (1976).

(78) L. Fanfani, A. Nunzi, P. F. Zanazzi, and A. R. Zanzari, *Acta Crystallogr., Sect. B*, **28**, 1298 (1972).

(79) J. A. Ibers, *Acta Crystallogr.*, **9**, 225 (1956).

(80) J. V. Silverton and J. L. Hoard, *Inorg. Chem.*, **2**, 243 (1963).

(81) H. Titze, *Acta Chem. Scand.*, **23**, 399 (1969); **24**, 405 (1970).

(82) R. P. Dodge, D. H. Templeton, and A. Zalkin, *J. Chem. Phys.*, **35**, 55 (1961).

(83) G. J. Bullen, *Acta Crystallogr.*, **12**, 703 (1959).

(84) E. L. Lippert and M. R. Truter, *J. Chem. Soc.*, 4996 (1960).

(85) F. A. Cotton and J. S. Wood, *Inorg. Chem.*, **3**, 245 (1964).

(86) (a) G. F. S. Wessels, J. G. Leipoldt, and L. D. C. Bok, *Z. Anorg. Allg. Chem.*, **393**, 284 (1972); (b) T. J. Pinnavaia, B. L. Barnett, G. Podolsky, and A. Tulinsky, *J. Am. Chem. Soc.*, **97**, 2712 (1975).

(87) (a) F. A. Cotton and J. G. Bergman, Jr., *J. Am. Chem. Soc.*, **86**, 2941 (1964); (b) J. G. Bergman, Jr., and F. A. Cotton, *Inorg. Chem.*, **5**, 1420 (1966).

(88) T. J. King, N. Logan, A. Morris, and S. C. Wallwork, *Chem. Commun.*, 554 (1971).

(89) J. G. Bergman, Jr., and F. A. Cotton, *Inorg. Chem.*, **5**, 1208 (1966).
(90) C. Bellito, L. Gastaldi, and A. A. G. Tomlinson, *J. Chem. Soc., Dalton Trans.*, 989 (1976).
(91) The related Sn^{IV} (ref 92) species seems to be closer to the Ti^{IV} (d^0) (ref 93) rather than the Zn (d^{10}) system. We shall regard it then as having a d^0 configuration.
(92) C. D. Garner, D. Sutton, and S. C. Wallwork, *J. Chem. Soc. A*, 1949 (1967).
(93) C. C. Addison, C. D. Garner, W. B. Simpson, D. Sutton, and S. C. Wallwork, *Proc. Chem. Soc., London*, 367 (1964).
(94) D. A. Langs and C. R. Hare, *Chem. Commun.*, 890 (1967).
(95) E. L. Muetterties, *Inorg. Chem.*, **4**, 769 (1965).
(96) E. L. Muetterties, *Acc. Chem. Res.*, **3**, 266 (1970).
(97) L. Malatesta, M. Freni, and V. Valenti, *Gazz. Chim. Ital.*, **94**, 1278 (1964).
(98) (a) R. C. Fay, D. F. Lewis, and J. R. Weir, *J. Am. Chem. Soc.*, **97**, 7179 (1975); (b) R. D. Archer and C. J. Donahue, *ibid.*, **99**, 269, 6613 (1977).
(99) R. C. Fay and J. K. Howie, *J. Am. Chem. Soc.*, **99**, 8110 (1977).
(100) J. P. Jesson, E. L. Muetterties, and P. Meakin, *J. Am. Chem. Soc.*, **93**, 5261 (1971).
(101) R. Hoffmann, *J. Chem. Phys.*, **39**, 1397 (1963); R. Hoffmann and W. N. Lipscomb, *ibid.*, **36**, 2179, 3489 (1962); **37**, 2872 (1962).
(102) H. Basch and H. B. Gray, *Theor. Chim. Acta*, **3**, 458 (1965).

Contribution from Le Laboratoire de Chimie des Organométalliques, ERA 477, Université de Rennes, 35031 Rennes Cedex, France, and The Guelph-Waterloo Centre for Graduate Work in Chemistry, Waterloo Campus, Department of Chemistry, University of Waterloo, Waterloo, Ontario N2L 3G1, Canada

Carbon Disulfide Complexes of Zerovalent Iron: Synthesis and Spectroscopic Properties. X-ray Crystal Structure of (η^2-Carbon disulfide)dicarbonyl(trimethylphosphine)(triphenylphosphine)iron(0)

HUBERT LE BOZEC,[1a] PIERRE H. DIXNEUF,*[1a] ARTHUR J. CARTY,*[1b] and NICHOLAS J. TAYLOR[1b]

Received August 18, 1977

Carbon disulfide complexes of iron(0), $Fe(\eta^2\text{-}CS_2)(CO)_2L_2$ [L = $P(OMe)_3$, $P(OEt)_3$, $P(OPh)_3$, PPh_3], have been synthesized from (benzylideneacetone)tricarbonyliron(0) via reaction with tertiary phosphorus ligands in carbon disulfide. An excellent route to the trialkyl- or dialkylarylphosphine complexes $Fe(\eta^2\text{-}CS_2)(CO)_2L_2$ (L = PMe_3, PMe_2Ph, $P(n\text{-}Bu)_3$) or $Fe(\eta^2\text{-}CS_2)(CO)_2(PPh_3)L$ (L = PMe_3, PMe_2Ph) consists of displacing one or two molecules of triphenylphosphine from $Fe(\eta^2\text{-}CS_2)(CO)_2(PPh_3)_2$ by the more nucleophilic phosphines. The mixed phosphine–phosphite derivative $Fe(\eta^2\text{-}CS_2)(CO)_2(PMe_3)(P(OMe)_3)$ can be obtained from $Fe(\eta^2\text{-}CS_2)(CO)_2(PMe_3)(PPh_3)$ via PPh_3 substitution. These compounds have been characterized by microanalyses, by IR, ^1H and ^{31}P NMR and mass spectroscopy, and for $Fe(\eta^2\text{-}CS_2)(CO)_2(PMe_3)(PPh_3)$ by single-crystal X-ray diffraction. Crystals of $Fe(\eta^2\text{-}CS_2)(CO)_2(PMe_3)(PPh_3)$ are monoclinic, space group *Pc*, with a = 9.309 (4) Å, b = 13.640 (12) Å, c = 11.390 (5) Å, β = 120.43 (5)°, and Z = 2. The structure was solved by Patterson and Fourier techniques using 1881 independent, counter-measured reflections for which $I \geq 3\sigma(I)$. Refinement by full-matrix least-squares methods with all nonhydrogen atoms having anisotropic thermal parameters converged at R = 0.039 and R_w = 0.046. The CS_2 ligand is η^2 coordinated and the iron stereochemistry is best described as trigonal bipyramidal with trans phosphorus ligands and the coordinated C=S bond of the CS_2 molecule occupying an equatorial position. Important bond lengths are C(3)–S(1) = 1.676 (7), C(3)–S(2) = 1.615 (8), Fe–S(1) = 2.334 (2), Fe–C(3) = 1.983 (8), Fe–P(1) = 2.279 (2), and Fe–P(2) = 2.252 (2) Å. The electronic nature of the bound CS_2 ligand is discussed in the light of structural and spectroscopic parameters.

Introduction

Transition-metal η^2-CS_2 complexes are the main precursors to thiocarbonyl compounds.[2a] The transformation of an η^2-CS_2 molecule to a thiocarbonyl is achieved either by removal of one sulfur atom as phosphine sulfide on treatment with a tertiary phosphine or via alkylation of the uncoordinated sulfur atom followed by alkylthiol elimination on subsequent reaction with acid[2a] or hydride ion[2b] (Scheme I). Moreover, η^2-CS_2 complexes are highly activated toward electrophilic reagents. The uncoordinated sulfur atom behaves as a strong nucleophile, displacing halide ion from alkyl halides to give sulfur alkylated cations[3] or weakly bound ligands from other organometallic derivatives leading to CS_2-bridged binuclear complexes.[4,5] Another interesting feature of CS_2 coordination chemistry concerns the electron-donor–electron-acceptor properties of this ligand. Recent spectroscopic evidence[6] may point to an acceptor capability for η^2-CS_2 in η^5-$C_5H_5Mn(CO)_2L$ complexes superior to that of CO and comparable with that of CS or PF_3.

Despite their synthetic utility and potential, relatively few η^2-CS_2 complexes of first-row transition metals have been characterized.[2a] We report herein the synthesis of a series of η^2-CS_2 complexes of the type $Fe(\eta^2\text{-}CS_2)(CO)_2LL'$ (L, L' = tertiary phosphine or phosphite) for which a versatile chemistry can be anticipated. The spectroscopic characterization of these complexes is described. An X-ray crystal structure analysis of $Fe(\eta^2\text{-}CS_2)(CO)_2(PMe_3)(PPh_3)$ has been carried out to provide the first accurate structural parameters for a first-row transition-metal CS_2 derivative and to form a basis for spectroscopic investigations of CS_2–M bonding.

Scheme I

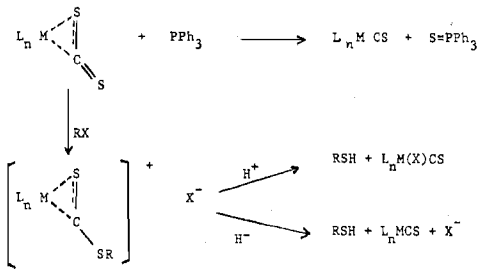

Experimental Section

General Methods. Infrared spectral determinations were made using a Beckman IR 12 spectrophotometer. Frequencies are accurate to ±2 cm^{-1}. NMR spectra were recorded on a Varian EM 360 (^1H; $CDCl_3$ solution with Me_4Si internal standard unless otherwise noted) and a Bruker WH 90 (^{31}P; $CDCl_3$ solution unless otherwise noted; shifts are downfield (+) from external H_3PO_4). Mass spectra were determined at 70 eV using a Varian MAT 311 double-focusing spectrometer. Microanalyses were determined by CNRS microanalyses (THIAIS).

Synthesis. $Fe(\eta^2\text{-}CS_2)(CO)_2[P(OR)_3]_2$ (2a (R = Me), 2b (R = Et), 2c (R = Ph)). The phosphite (2 mmol) was added to a solution of (benzylideneacetone)tricarbonyliron (**1**)[7] (1 mmol) in CS_2 (5 mL)

